# Heterogeneity of the chemical composition and thermal stability of particulate organic matter in French forest soils

Laure Soucémarianadin, Lauric Cécillon, Claire Chenu, François Baudin, Manuel Nicolas, Cyril Girardin, Amicie Delahaie, Pierre Barré

# Heterogeneity of the chemical composition and thermal stability of particulate organic matter in French forest soils

Laure Soucémarianadin[1,*], Lauric Cécillon[1,2], Claire Chenu[3], François Baudin[4], Manuel Nicolas[5], Cyril Girardin[3], Amicie Delahaie[1] and Pierre Barré[1]

[1] Laboratoire de Géologie, PSL Research University, CNRS-ENS UMR8538, Paris, France

[2] Université de Normandie, UNIROUEN, IRSTEA, ECODIV, 76000 Rouen, France

[3] UMR ECOSYS, INRA, AgroParisTech, Université Paris-Saclay, 78850 Thiverval-Grignon, France

[4] Sorbonne Université/CNRS, UMR ISTeP, 4 place Jussieu 75005 Paris, France

[5] Office National des Forêts, R&D, 77300 Fontainebleau, France

* Corresponding author: Laure Soucémarianadin, souce@geologie.ens.fr

Laboratoire de Géologie (UMR 8538) Ecole Normale Supérieure, 24 Rue Lhomond 75231 Paris CEDEX 5, France; phone: +331 44 32 22 94; fax: +331 44 32 22 00

Type: Regular article

**Abstract**

In temperate forests, soils contain a significant part of the ecosystem carbon (C) stock that can be subjected to C losses upon global changes. In forest soils, particulate organic matter (POM) is a major contributor to the labile C pool and its dynamics can significantly influence the overall total soil organic carbon stock. However, POM has been overlooked in forest soils, specifically in deep horizons.

We isolated the POM fraction of mineral soil samples collected in 52 French forest sites, using a size- (> 50 µm) and density- (< 1.6 $g \cdot cm^{-3}$) fractionation scheme. These soil samples presented variability in terms of depth (0–10 cm; 40–80 cm), soil class (dystric Cambisol, eutric Cambisol, entic Podzol) and vegetation type (deciduous, coniferous). First, we determined the POM chemical composition and thermal stability using elemental analysis, mid infrared-attenuated total reflectance spectroscopy and Rock-Eval thermal analysis. Then, we assessed how depth, soil class and vegetation type influenced POM chemistry and thermal stability in these temperate forest soils.

Depth, soil class and vegetation type were all important factors influencing POM chemistry and thermal stability. Variations in POM chemistry (higher C/N ratio, lower ether + alcohol and carbonyl + carboxyl ratios and decrease in hydrogen-rich compounds) and increase in thermal stability with depth suggested different POM input sources for the surface and deep soil layers and an increased biogeochemical stability of POM in deep soil layers. Whatever the vegetation, POM in eutric Cambisols had lower aliphatic and higher aromatic ratios than POM in dystric Cambisols. POM in soils under deciduous trees had higher aliphatic and carbonyl + carboxyl ratios and lower aromatic ratio, more hydrogen-rich and less oxygen-rich compounds than POM in soils under coniferous trees, reflecting the difference in litter chemistry between the two vegetation types. POM from deciduous plots was also significantly

more thermally stable than from coniferous plots, suggesting a higher biogeochemical stability for POM in deciduous forest soils.

This study highlights the variations in POM chemistry and thermal stability existing within and among soil profiles and the role of depth, soil class and vegetation type in these variations. It appears that if POM can be regarded as a labile carbon fraction in soils, its lability varies depending on the ecosystem (soil, vegetation) and depth considered.

**Keywords**: forest soils; soil organic carbon stability; particulate organic matter; Rock-Eval; mid-infrared spectroscopy; environmental drivers.

**Abbreviations**: Rock-Eval 6 (RE6), particulate organic matter (POM), mid-infrared-attenuated total reflectance (MIR-ATR)

## 1. Introduction

Soil organic carbon (SOC) is made up of very heterogeneous compounds (Trumbore, 1997; Amundson, 2001) with turnover times ranging from a few days/weeks to several centuries. The most labile SOC pools are very sensitive to environmental changes (Carter et al., 1998; Zhang et al., 2007), which could result in rapid variations of SOC stocks (~years) and as such they play an important role in global warming and its mitigation. Labile SOC is also central to short-to medium-term nutrient availability and soil structural stability (Wander, 2004). The particulate organic matter (POM) fraction represents a labile SOC pool constituted of partially decomposed organic debris, *i.e.*, plant and animal residues, (Spycher et al., 1983; Christensen, 1992) with a mean residence time that is usually considered to be < 20 years for temperate *in-situ* conditions (e.g., Trumbore et al., 1996; Balesdent, 1996). POM fractions are separated and quantified as low-density and/or coarse-size fractions (often > 50–250 μm; Wander, 2004). POM is primarily a source of energy and C for microbial decomposers and soil fauna but is also a source of N and other nutrients (Haynes, 2005). POM fractions are typically enriched in carbohydrates relative to whole soils and heavy fractions (Baldock et al., 1992; Baldock et al., 1997) with carbohydrates representing 5 to 25% of the C in the POM fraction (Oades, 1972; Oades et al., 1987). The elemental composition of POM also plays a major role in its dynamics and organic materials with higher N content (low C/N ratio) tend to decompose faster than those with low N content (Swift et al., 1979; Aber and Melillo, 1980; Melillo et al., 1982; Cotrufo et al., 1995).

Soils experiencing conditions that will limit decomposition (*e.g.*, cold and dry climates or low pH) and that are under permanent vegetation allowing for high inputs of aboveground and belowground plant litter (*e.g.*, forests and permanent grasslands) will tend to favour POM accumulation (e.g., Whitehead et al., 1975; Balesdent et al., 1998; Leifeld et al., 2009). In agricultural soils, the POM fraction contains 2–18% of total SOC and 1–16% of total soil N

(Gregorich and Janzen, 1996). In forest topsoils, the POM fraction represents 5–47% of total SOC and 3–40% of total soil N (Christensen, 1992). Variations in SOC stocks after land-use change have been largely associated to C gains or losses in the POM fraction (Poeplau and Don, 2013).

Some studies have investigated the effects of environmental factors on POM properties. POM quantity and chemistry have been shown to vary according to vegetation (Quideau et al., 2001; Laganière et al., 2011; Schrumpf et al., 2013) or parent material/soil type (Kölbl and Kögel-Knabner, 2004; Angst et al, 2018). However, these studies often lack multi-site observations. And despite their importance for SOC dynamics and soil quality, POM fractions from surface and deep horizons of forest soils remain poorly documented.

Mid-infrared (MIR) spectroscopy can provide information related to soil chemical composition as most chemical bounds found in soil minerals and organic compounds have spectral absorptions at specific wavelengths of the IR domain (Nguyen et al., 1991). The chemical characterization of soil organic matter (SOM) in bulk soils by MIR spectroscopy is made difficult because of mineral interferences (Nguyen et al., 1991; Reeves, 2012; Cécillon et al., 2012), while the characterization of pure SOM fractions does not suffer this caveat. The MIR technique in the attenuated total reflectance mode (MIR-ATR) has been used to describe the chemical composition of pure SOM in Histosols (Pengerud et al., 2013; Robroek et al., 2015) or to study the bulk chemistry of the POM fractions in mineral soils (Puissant et al., 2017).

Among thermal analyses used to characterize SOM, Rock-Eval (RE) analysis has provided promising results showing that SOC thermal stability observed in RE thermograms results can be related to SOC biogeochemical stability (Gregorich et al., 2015; Saenger et al., 2015; Barré et al., 2016; Soucémarianadin et al., 2018a; Poeplau et al., 2019). RE was also shown to provide information on organic matter evolutions in soils at various depth or during

composting (Hetényi et al., 2005; Hetényi et al., 2006; Sebag et al., 2006; Albrecht et al., 2015), and it has been specifically applied to characterize litters, bulk soil, organic layers and POM fractions in mineral soils (Disnar et al., 2003; Saenger et al., 2015; Sebag et al., 2016).

The objectives of this study were thus to characterize POM chemistry and thermal stability in a set of French forest soil samples and then to assess the importance of various environmental factors, namely soil depth, soil class and vegetation type in controlling POM chemistry and thermal stability. To this purpose, we separated by size and density the POM fraction from a set of French forest soil samples that covers a large pedoclimatic variability as well as tree species diversity and includes deep samples (up to 0.8 m). We then used a set of complementary techniques (*i.e.*, C and N elemental analysis, MIR-ATR spectroscopy and RE thermal analysis) to characterize POM chemistry and thermal stability.

We hypothesized that 1/ vegetation type (coniferous *vs.* deciduous dominant canopy trees) affects POM chemistry and thermal stability. Specifically we expected POM from coniferous trees to have more aromatic moieties because of their (likely) higher lignin content (Berg et al., 2013) but a lower thermal stability than POM from deciduous plots, at least in the surface layer. Deciduous forests have a more rapid plant-soil nutrient cycling than coniferous forests (Cole and Rapp, 1981) and litter is decomposed faster. In parallel, more decomposed organic matter has been shown to have higher thermal stability (Disnar et al. 2003); 2/ eutric Cambisols provide higher physical protection to POM than the two other soil classes due to their higher calcium (Rowley et al., 2018) and clay contents (Kölb and Kögel-Knabner, 2004). This could result in lower thermal stability for POM in eutric Cambisols; and 3/ depth influences POM C/N ratio, increasing with depth as POM would be likely more decomposed in surface than in the deep layer due to more favourable environmental conditions and a greater contribution of partially decomposed leaf litter.

## 2. Material and methods

### 2.1. Sampling

Mineral soils samples were collected in 52 forest sites of the French national network for the long term monitoring of forest ecosystems (‘‘RENECOFOR’’). These permanent plots were established in 1992 (Ulrich, 1995) by the National Forest Service (ONF) and are part of the European network ICP-FORESTS level 2 (Fig. 1a). Details regarding these sites have been previously published (Soucémarianadin et al., 2018b). Briefly, they presented variability in terms of soil type with a class constituted of soils related to entic Podzols, another class constituted of eutric and epileptic Cambisols as well as a few Calcisols and a last class constituted of dystric and hyperdystric Cambisols (IUSS Working Group, 2015). Forest vegetation varied also among sites, with coniferous [silver fir (*Abies alba* Mill.); Norway spruce (*Picea abies* (L.) H. Karst.); European larch (*Larix decidua* Mill.); Scots pine (*Pinus sylvestris* L.)] and deciduous [beech (*Fagus sylvatica* L.); sessile (*Quercus petraea* (Matt.) Liebl.) and/or pedunculate oaks (*Quercus robur* L.)] stands. Finally, the sites also varied in terms of climate (continental influence, oceanic influence, mountainous influence; with mean annual precipitation = 703–1894 mm and mean annual temperature = 4.8–12.3 °C for the 1971–2000 period). Samples representing two mineral soil layers were obtained (0–10 cm = topsoil and 40–80 cm = subsoil; Fig. 1b) at each site. Samples of the topsoil layer were composite of 5 × 5 sampling points and were collected by digging a 50 cm wide soil profile (Ponette et al., 1997; Jonard et al., 2017). Samples of the deep soil layer (subsoil) were composite from two soil pits (Brêthes et al., 1997).

Samples storage and pooling have been detailed elsewhere (Soucémarianadin et al., 2018a). The pooled samples were sieved at 2 mm before analysis.

## 2.2. Particle size and density SOC fractionation

The protocol builds on that of Balesdent et al. (1991) combining both size and density separation. Because our protocol involved both density and size fractionation, we chose to refer to the isolated fraction as the particulate organic matter (POM) fraction (and not just light fraction).

Details regarding the POM fraction isolation procedure have been previously published (Soucémarianadin et al., 2018a). Briefly 25 g of samples were shaken overnight in a 0.5% sodium hexametaphostate solution with ten 5 mm-diameter glass beads. Samples were thoroughly rinsed over a 50-µm mesh with deionized water. The sand fraction (> 50 µm) was then mixed with a sodium polytungstate (SPT) solution of density = 1.6 ± 0.03 $g \cdot cm^{-3}$ shaken and left to settle down overnight. We collected the floating material with a spatula and placed it over a 50-µm mesh sieve. If material was still found floating, SPT solution was added back to the flask and the previous step was repeated using centrifugation for 30 minutes (2750 rpm) to accelerate the separation, as many times as needed until nothing was left floating. As soon as the POM fraction was added to the sieve, it was thoroughly rinsed using deionized water, and this was repeated throughout the whole process. We relied on a visual check (after drying; magnification ×10) of the POM material and the sieve for residual traces of SPT. In case traces of salt were observed the sample was again thoroughly rinsed with deionized water, dried and checked one more time. The sieves and fractions were then placed in the oven at 50 °C for 24 h before being weighed. POM fractions were further ground with a ball mill (mixer mill MM 200, Retsch Gmbh) or a mortar and pestle when the sample mass was less than 0.05 g.

A total of 102 samples were initially fractionated for POM. However, some samples still contained traces of SPT as shown by their low C content (≤ 30%) and/or MIR-ATR spectra (see section 2.4.) and because we were concerned with possible interactions altering the

thermal analysis signals, they were thus excluded from the statistical analysis. This resulted in the exclusion of 16 samples, (n = 6) for the 0–10 cm soil layer and (n = 10) for the 40–80 cm soil layer, leaving a total of 86 samples.

### 2.3. Elemental analysis

Organic carbon and total nitrogen concentrations of the ground POM fractions were determined by dry combustion with an elemental analyzer (CHN NA 1500, Carlo "Elba"). Using these concentrations we determined the C/N ratio of the POM samples.

### 2.4. Mid-infrared spectroscopy

The chemical composition of the POM OC was further assessed by Fourier transform mid-infrared-attenuated total reflectance (MIR-ATR) spectroscopy. Prior to analysis, the ground samples were dried overnight at 40 °C to standardize their water content without altering organic matter chemistry.

MIR-ATR spectra were acquired with a Nicolet *iS10* infrared spectrometer (Thermo Fischer Scientific Inc., Madison, WI, USA) equipped with an ATR device (diamond crystal) over the spectral range 4000–650 $cm^{-1}$, with a spectral resolution of 4 $cm^{-1}$ and 16 scans. All spectra were corrected for atmospheric interferences ($H_2O$ and $CO_2$). Absorbance was calculated as the inverse logarithm of the measured reflectance.

Pre-processing of the spectra included a systematic offset-correction, which shifted individual spectrum to set the *y*-minimum to zero (Bruker, 2011), using the 4000–3950 $cm^{-1}$ region as a reference.

Four spectral regions, adapted from Puissant et al. (2017), corresponding to specific C functional groups were used to characterize POM chemistry: (1) the aliphatic ($CH_2$ and $CH_3$ stretch) region between 2950–2900 $cm^{-1}$; (2) the carbonyl and carboxyl (C=O stretch) region

between 1750–1690 $cm^{-1}$; (3) the aromatic C (C=C bond) region between 1605–1575 $cm^{-1}$ and (4) the ether and alcohol (C-O stretch typically found in carbohydrates) region between 1180–1145 $cm^{-1}$ (Fig. A.1). Relative ratios for these four regions were then calculated using Eq. 1:

Relative ratio (region *i*) = (area region *i*)/$\sum$ (areas of 4 regions)) (Eq. 1)

The contribution of soil minerals (*e.g.* phyllosilicates) or SPT pollution to the intensities of the four waveband-regions was negligible for the 86 selected POM fractions. The potential pollution of POM fractions with SPT was tested by comparing all POM MIR-ATR spectra to the spectrum of pure SPT powder and making sure that there were no over-average peaks, specifically for the two peaks centered around 720 $cm^{-1}$ and 860 $cm^{-1}$. These two peaks are high intensity and well-defined in the pure SPT powder spectrum but not apparent in most POM spectra. Therefore the presence of peaks centered on these two wavelengths indicated the possibility of SPT contamination and these samples were thus excluded (see section 2.2.). Signal processing of the MIR-ATR spectra was performed with the R environment software v.3.3 (R Core Team, 2016) using the pracma (Borchers, 2015) and hyperSpec (Beleites and Sergo, 2015) R packages.

### 2.5. Thermal analysis: Rock-Eval 6

Samples were also analysed with a Rock-Eval 6 turbo device (Vinci Technologies, France; Behar et al., 2001). We modified the procedure developed for the analysis of SOM by Disnar et al. (2003) as detailed in Soucémarianadin et al. (2018b). Briefly, about 10 mg of ground sample mixed with 50 mg of ground Fontainebleau sand (previously muffle-furnaced at 850 °C for 15 minutes to ensure that it was C-free) were exposed to two consecutive thermal treatments. Samples were first introduced in a pyrolysis oven (under $N_2$ atmosphere) then in a combustion oven (under laboratory air atmosphere). The pyrolysis began with an isothermal

step (at 200 °C) that lasted around 200 seconds and during which the free hydrocarbons (HC) were thermovaporized (S1 peak). A flame ionization detector allowed for the quantification of the pyrolysis effluents (mostly HC), while an infrared detector quantified CO and $CO_2$ during both the pyrolysis and oxidation stages (Fig. A.2).

Two standard RE6 parameters were determined: the hydrogen index (HI; mg HC·$g^{-1}$ TOC) and the oxygen index ($OI_{RE6}$; mg $O_2$·$g^{-1}$ TOC). HI corresponds to the quantity of pyrolyzed relative to the total organic carbon content of the sample and describes the relative enrichment/depletion of POM in hydrogen-rich moieties. $OI_{RE6}$ corresponds to the oxygen yield as CO and $CO_2$ during the thermal pyrolysis divided by the total organic carbon content of the sample. It describes the relative oxidation status of POM. In this study, as POM does not contain inorganic C, we corrected the calculation of HI (HI corrected; expressed as mg HC·$g^{-1}$ OC) to consider all the C signals (TOC and MinC) as organic C. This did not change drastically the values (Table B.1). This corrected HI value is simply referred to as HI hereafter.

We derived one additional RE6 parameter describing the thermal stability of POM: $T_{50\_CO2\_PYR}$, the temperature at which 50% of the $CO_2$ resulting from organic matter pyrolysis had evolved. Because the signal was noisy at the beginning of the pyrolysis, we started the integration for $T_{50\_CO2\_PYR}$ right after the S1 peak. This $T_{50}$ temperature parameter and the HI index have been previously shown as good thermal indicators of SOM biogeochemical stability (Barré et al., 2016; Cécillon et al., 2018). While HI decreased with time since bare-fallow and with the proportion of persistent SOC in a soil sample, $T_{50\_CO2\_PYR}$ increased (Barré et al., 2016; Cécillon et al., 2018). The latter also appeared as the most important thermal parameter to predict the proportion of persistent SOC with a multivariate model (Cécillon et al., 2018). As such, $T_{50\_CO2\_PYR}$ could be considered as an indicator of C persistence in soils.

Signal processing of the RE6 thermograms (signal integration and calculation of the $T_{50}$ temperature) was performed with the R environment software v.3.3 (R Core Team, 2016) using the hyperSpec (Beleites and Sergo, 2015) and pracma (Borchers, 2015) R packages.

### 2.6. Calculations and statistical analyses

Although our design was not truly balanced, the distribution of our 86 samples, representing 52 plots (Fig. 1b), among the classes of the various environmental factors (depth, soil class and vegetation type) was not too biased (Table C.1).

The statistical analysis to determine the driving factors of POM chemistry was performed in a similar manner as previously published for the SOC stability of the bulk mineral soil (Soucémarianadin et al., 2018b). Briefly, we used multivariate models to assess the effects of the three environmental factors (depth, soil class and vegetation type) on the different POM chemistry and thermal stability parameters. The linear mixed models introduced a random intercept for each site (≈ to treat "site" as random effect) to take into account that the two layers constituted repeated measures (increasing depth within a same RENECOFOR site). To do so, we added the compound symmetry structure to a generalized least squares (gls) function. The latter fits a linear model using generalized least squares (Pinheiro et al. 2016). Model selection was then implemented with a top-down strategy for optimal fit with the restricted maximum likelihood (REML) approach. The response variables were transformed, to the exception of $T_{50\_CO2\_PYR}$, using a reciprocal transformation or the Box-Cox transformation technique, as they showed evidence of the variance increasing with the mean response. After transformation, all residuals followed a normal distribution. We relied on the Cook's distance to identify potential outliers.

All comparisons were considered significant at an alpha value ($\alpha$) of 0.05.

Relationships between the parameters related to POM chemistry and parameters linked to thermal stability were estimated using Spearman rank correlation as the data did not meet the assumption of normality. All statistical analyses were performed using the R 3.3 statistical software (R Core Team, 2016) with the nlme (Pinheiro et al., 2016), lme4 (Bates et al., 2015) and car (Fox and Weisberg, 2011) packages.

# 3. Results

The effects of climate were tested in a preliminary analysis but this factor (or its interactions with other factors) never had a significant influence on parameters of POM chemistry and thermal stability. We thus decided not to present the results here for concision sake.

## 3.1. Heterogeneity of POM chemistry

### 3.1.1. Effects of vegetation type

Vegetation type was highly significant for all parameters except for C/N ratio and MIR-ATR ether + alcohol ratio (Table 1). When comparing the three other MIR-ATR-derived ratios in our 52 sites, POM in deciduous plots had higher aliphatic and carbonyl + carboxyl ratios and lower aromatic ratio (0.191 ± 0.016, 0.220 ± 0.031 and 0.239 ± 0.048, respectively) than the POM found in soils from coniferous plots (0.181 ± 0.009, 0.207 ± 0.021 and 0.268 ± 0.030, respectively; Table 2).

### 3.1.2. Effect of soil class

Soil class was highly significant for all parameters except for both the MIR-ATR aromatic ratio and ether + alcohol ratio (Table 1). In our sample set, when differences were observed among soil classes, the general trend was that a given parameter (C/N ratio, aliphatic and carbonyl + carboxyl ratios) was lower in POM from eutric Cambisols (34 ± 7; 0.178 ± 0.010;

310 0.190 ± 0.020, respectively) than in POM from dystric Cambisols (42 ± 14; 0.192 ± 0.016;
311 0.226 ± 0.023, respectively; Table 2). Values of these parameters for the POM in entic
312 Podzols were lower than for the POM in dystric Cambisols but still significantly greater than
313 for the POM in eutric Cambisols (Table 2).

314 3.1.3. Effect of soil depth

315 The effect of depth was significant for all parameters of POM chemistry except the aliphatic
316 ratio (Table 1). The MIR-ATR ether + alcohol and carbonyl + carboxyl ratios significantly
317 decreased with depth (0.357 ± 0.019 to 0.336 ± 0.017 and 0.221 ± 0.025 to 0.204 ± 0.026,
318 respectively), while the aromatic ratio significantly increased (0.236 ± 0.038 to 0.274 ± 0.038;
319 Table 2). The C/N ratio also increased from 30 ± 8 in the surface layer to 48 ± 11 in the deep
320 layer (Table 2).

321 3.1.4. Factor interactions

322 Depth × soil was the most common significant interaction (C/N ratio, aliphatic ratio and
323 aromatic ratio), followed by soil × vegetation (aromatic ratio and carbonyl + carboxyl ratio)
324 and depth × vegetation (carbonyl + carboxyl ratio; Table 1). By looking closely at these
325 interactions, different patterns were observed.

326 Soil class was an important driver of POM chemistry through its interactions with both depth
327 and vegetation type, with the effects of these two environmental drivers being generally
328 buffered in eutric Cambisols. Specifically there was no effect of vegetation type on aromatic
329 ratio and carbonyl + carboxyl ratio in eutric Cambisols (Fig. D.1). Moreover, for these two
330 ratios, differences among soil classes were smaller under the coniferous vegetation (Fig. D.1).
331 Similarly, the differences between the surface and deep layers in C/N ratio, aliphatic ratio and
332 aromatic ratio were reduced in eutric Cambisols compared with the two other soil classes
333 (Fig. 2). If there was no overall effect of depth on the aliphatic ratio of POM, opposite trends
334 were found in dystric Cambisol (decrease) and entic Podzol (increase) with depth (depth ×

soil interaction; Fig. 2). For the C/N ratio, it appeared that the soil effect was mainly due to differences in the deep layer (Fig. 2). Finally, for the carbonyl + carboxyl ratio, the depth effect was not observed in the deciduous plots (Fig. 3).

### 3.2. Heterogeneity of POM Rock-Eval thermal parameters

#### 3.2.1. Effect of vegetation type

Vegetation type significantly influenced all parameters of POM thermal parameters (Table 1). HI and $T_{50\_CO2\_PYR}$ were higher in POM of soils under deciduous trees (346 ± 88 mg $HC \cdot g^{-1}$ OC and 358 ± 10 °C, respectively) than coniferous trees (213 ± 59 mg $HC \cdot g^{-1}$ OC and 355 ± 8 °C, respectively; Table 2), while $OI_{RE6}$ was significantly lower (166 ± 42 mg $O_2 \cdot g^{-1}$ TOC *vs.* 194 ± 26 mg $O_2 \cdot g^{-1}$ TOC; Table 2).

#### 3.2.2. Effect of soil class

HI and $T_{50\_CO2\_PYR}$ were significantly lower in POM from eutric Cambisols (244 ± 87 mg $HC \cdot g^{-1}$ OC and 351 ± 5 °C, respectively) than from dystric Cambisols (305 ± 114 mg $HC \cdot g^{-1}$ OC and 360 ± 10 °C) and entic Podzols (Table 2). Conversely, $OI_{RE6}$ was higher in POM from eutric Cambisols (214 ± 30 mg $O_2 \cdot g^{-1}$ TOC) than from entic Podzols and dystric Cambisols (171 ± 27 and 158 ± 29 mg $O_2 \cdot g^{-1}$ TOC, respectively; Table 2).

#### 3.2.3. Effect of soil depth

The effect of depth was significant for HI and $T_{50\_CO2\_PYR}$ but not for $OI_{RE6}$ (Table 1). It is worth noting that the variability of $OI_{RE6}$ was however greater in the deep layer (sd = 45 mg $O_2 \cdot g^{-1}$ TOC *vs.* sd = 29 mg $O_2 \cdot g^{-1}$ TOC in the surface layer; Table 2) and overshadowed the slight increase with depth.

HI decreased from 301 ± 86 mg $HC \cdot g^{-1}$ OC in the surface layer to 248 ± 108 mg $HC \cdot g^{-1}$ OC in the deep layer (Table 2). $T_{50\_CO2\_PYR}$ was higher in the deep layer (363 ± 9 °C) than in the

surface layer (351 ± 5 °C; Table 2), indicating an increase in thermal stability of the POM fraction with depth.

#### 3.2.4. Factor interactions

Depth × soil ($T_{50\_CO2\_PYR}$), soil × vegetation ($OI_{RE6}$) and depth × vegetation (HI) were all significant interactions (Table 1). For $T_{50\_CO2\_PYR}$, the soil effect was mainly due to differences in the deep soil layer (Fig. 2). For $OI_{RE6}$, the vegetation effect was not significant in eutric Cambisols (Fig. D.1). For HI, the depth effect was not observed in the deciduous plots (Fig. 3).

## 4. Discussion

### 4.1. Influence of vegetation type on POM chemistry and thermal stability

Results from the literature were generally consistent with our findings of POM of deciduous origin having more aliphatic and carbonyl/carboxyl and less aromatic C than POM of coniferous origin. Using $^{13}C$ CP/MAS NMR, Preston et al. (2000) found significantly more aromatic and phenolic C in foliar litters of coniferous species than deciduous species, supporting other studies that showed that deciduous species tend to have lower concentrations of lignin than coniferous species (Berg et al., 2013). With the same technique, Rumpel et al. (2002) observed a greater proportion of alkyl-C in beech than spruce roots sampled from deep layer (B horizons), and these authors suggested that suberin might be an important contributor of the alkyl-C. As the percentage of fine root biomass in the first 30 cm of soil is higher in deciduous temperate forests than their coniferous counterparts (Jackson et al., 1997), this could at least partially explain our higher MIR-ATR carbonyl + carboxyl ratio in the deciduous POM. Both the aliphatic and carbonyl + carboxyl ratios of deciduous POM had a variability that was much larger than for the coniferous POM and illustrate the fact that inter-

384 species differences are important when it comes to plant chemistry (Berg and McClaugherty,
385 2013). Further studies looking at species level are therefore warranted.
386 In our study plots, HI and $T_{50\_CO2\_PYR}$ were significantly higher in POM of soils under
387 deciduous trees than coniferous trees (Table 2) while $OI_{RE6}$ was significantly lower (Table 2).
388 As coniferous litter is generally considered more difficult to decompose (e.g., Prescott, 2010),
389 we would have expected a higher $T_{50\_CO2\_PYR}$ for the POM in coniferous plots. When looking
390 more closely, the difference in $T_{50\_CO2\_PYR}$ between the two vegetation types originated
391 mainly from the surface layer (Fig. 3). This difference in thermal stability of the POM
392 between the two vegetation types might be related to a higher turnover in deciduous plots
393 (Cole and Rapp, 1981; Quideau et al., 2001) and/or, in coniferous plots, to a protection from
394 decomposition due to complexation of root tissues and litter with Al and Fe (Rasse et al.,
395 2005). Previous study of the thermal stability of total SOC in these forest sites
396 (Soucémarianadin et al., 2018b) showed that total SOC was also more thermally stable in the
397 surface layer of deciduous plots than coniferous plots. Overall, these results only partially
398 validated our first hypothesis, as we were not able to highlight that POM in soils under
399 deciduous trees was in fact more decomposed.
400 The absence of a vegetation effect on the POM C/N ratio could be explained by previous
401 observations in soils under deciduous than in coniferous species. If, for our study species, the
402 C/N ratio of fresh foliage found in the literature appear much lower in deciduous than in
403 coniferous species (Cools et al., 2014), the C/N ratio of organic layers did not significantly
404 differ between the deciduous ($30 \pm 6$) and coniferous plots ($31 \pm 7$) in our study sites (Brêthes
405 et al., 1997). POM in topsoil is more likely to derive from the organic layers than directly
406 from fresh leaves/needles.
407
408 4.2. Influence of soil class on POM chemistry and thermal stability

In our study sites, POM from eutric Cambisols was significantly different from POM from dystric Cambisols and entic Podzols. Using $^{13}C$ NMR spectroscopy and elemental analysis, Kölbl and Kögel-Knabner (2004) reported a protection of POM by clay through higher aggregation, leading to a less decomposed POM (higher C/N and O-alkyl and lower aryl C) in a clayey soil compared with a sandy soil. Yeasmin et al. (2017) observed variations in the chemical composition of POM ($d < 1.8\ g \cdot cm^{-3}$) among four soil types, using elemental analysis and MIR spectroscopy in the diffuse reflectance mode. Specifically, POM in their clayey soil had higher C/N ratio than in the other soil types and POM in the sandy soil had a large aliphatic C band compared with POM in the clayey soil. These results contradict our own observations as POM in eutric Cambisols (clay content = 37 ± 11%; Soucémarianadin et al. 2018b) had lower C/N ratio than POM from dystric Cambisols and entic Podzols (clay content = 18 ± 9% and 15 ± 9%, respectively). However, they agree with the lower aliphatic and carbonyl + carboxyl ratios we observed in eutric Cambisols. Yeasmin et al. (2017) also reported only small (non-significant) differences in the aromatic spectral region and no difference for the ether + alcohol band of POM among the four soil types, similar to our results. Finally, comparing soils with clay content varying between 12% and 72%, Golchin et al. (1994) did not either observe a clear trend on POM C/N ratio or chemical composition with soil texture.

When combining the differences in POM chemistry we observed in eutric Cambisols compared with dystric Cambisols and entic Podzols, with the differences in thermal parameters (lower HI and higher $OI_{RE6}$ in POM from eutric Cambisols), our results suggest that POM in eutric Cambisols is more decomposed than in dystric Cambisols and entic Podzols. This contradicts the lower $T_{50\_CO2\_PYR}$ values observed in eutric Cambisols but it appears that the significant difference in thermal stability among soil classes are only present in the deep layer (Fig. 2), while differences in HI were mainly found in the surface layer.

Overall, our results thus disprove our second hypothesis. One possible explanation could be that as eutric Cambisols have a greater water availability (Brêthes et al., 1997) and more nutrient exchange sites (cation exchange capacity = 24.4 ± 12.3 cmol(+)/kg) as well as a higher pH (Soucémarianadin et al., 2018b), this could promote decomposition. Moreover, there could be a threshold value for clay content to determine whether it promotes or reduces decomposition and clay mineralogy is also likely to affect decomposition (Fissore et al., 2016). Our result call for a more in-depth characterization of the chemical nature of the POM from the different soil classes (maybe using $^{13}C$ NMR) to further explain the variations observed among classes. Although as previously mentioned, our design was not overall too unbalanced, it should finally be noted that soil and vegetation appeared as confounded factors in our design. POM from coniferous plots was found preferentially on Podzols (70%), while POM from deciduous plots was preferentially associated with eutric Cambisols (59%). These unbalances could have affected our results and prevented us from properly discriminating the effects of vegetation *vs.* soil on POM characteristics in our study sites.

### 4.3. Contrasting POM chemistry and thermal stability at various soil depths suggests different C input sources

The increase in POM C/N ratio with depth was consistent with previous observations in forest ecosystems (Spycher et al., 1983; Schrumpf et al., 2013). The ether + alcohol and carbonyl + carboxyl ratios are considered as representative of labile C compounds (Baldock et al., 1992; Sarkhot et al., 2007; Ng et al., 2014) and their observed decrease with depth could correspond to the decomposition of POM from the surface to the deep layer (Baldock et al., 1997). Similarly, with depth, HI decreased while $T_{50\_CO2\_PYR}$ increased: these opposite trends match what is generally observed for bulk soil OC and organic material (Disnar et al., 2003; Sebag et al., 2016; Soucémarianadin et al., 2018a). These evolutions have been linked to an

increased decomposition and a decrease in labile C compounds, resulting in a more thermally and biogeochemically stable OC (Sebag et al., 2006; Albrecht et al., 2015; Barré et al., 2016; Cécillon et al., 2018). Our results for the thermal parameters could thus suggest a more decomposed POM in the deep layers.

However, if POM in the deep layers were more decomposed we would have expected a decrease of the C/N ratio. The fact that the latter was significantly higher in the deep layers would hint at the fact that the differences in chemistry between POM from the surface and deep layers originated from variations in POM sources. The high C/N ratios observed in the deep layers matched a higher contribution of roots compared to leaf litter in the deep layers. C/N ratios of fine roots are closer to 50–60 (Hobbie *et al.*, 2010) and even higher (Angst et al., 2016), while C/N ratios of fresh foliage or humus layers range between 15 and 45 (Brêthes et al., 1997; Disnar et al., 2003; Cools et al., 2014). Roots tend to have higher lignin content than leaves, which could explain the increase in the aromatic ratio (Natelhoffer and Fry, 1988; Berg and McClaugherty, 2013). This difference in main sources of POM could also explain the decrease of HI with depth. There are variations of HI values among plant organs, with "woody" materials tending to have lower HI. For instance, high HI values have been observed for needles or OL horizons of deciduous forest floors (≈ 300; Disnar et al., 2003; Sebag et al., 2006; Carrie et al., 2012), while bark HI was only 140 mg $HC \cdot g^{-1}$ TOC (Carrie *et al.*, 2012). The observed increase of $T_{50\_CO2\_PYR}$ in the POM fraction of the deep layer could also be related to the fact that the deeper POM comes from a different source that is more stable (*i.e.*, woody roots *vs.* leaves and needles litter). This could also explain the increase in the aromatic ratio (Kögel-Knabner, 2002). These results thus confirmed our third hypothesis. The lack of correlation between HI and $T_{50\_CO2\_PYR}$ (Table E.1) supports this hypothesis of different POM inputs between the two layers rather than just a decomposition gradient. Soil class and

vegetation type were also important factors, confirming combined effects of input quality and decomposition for POM chemistry and thermal stability.

### 4.4. Some POM are more labile than others

The strong heterogeneity we observed in the POM samples of our 52 forest sites suggest that POM lability varies. All the chemical (higher C/N ratio and aromatic ratio, lower ether + alcohol and carbonyl + carboxyl ratios) and thermal (higher $T_{50\_CO2\_PYR}$ and lower HI) properties of deep layer POM point towards a more labile POM in the topsoil than subsoil. Aryl C is considered as relatively stable carbon forms (Ng et al., 2014), while carbonyl C is considered as more labile C (Sarkhot et al., 2007; Ng et al., 2014). The moderate to strong positive correlation between C/N ratio and $T_{50\_CO2\_PYR}$ (Table E.1) suggested that POM with higher C/N ratios were more thermally (and biogeochemically) stable. This could be linked to previous reports showing that litters with low C/N ratio are more easily decomposed (Cotrufo et al., 1995), thus connecting thermal and chemical indicators of biogeochemical stability. Free POM (light fraction) turnover has been shown to increase by an order of magnitude from the 0–5 cm layer (turnover < 10 years) to the 10–20 cm layer (turnover ≈ 100 years) (Schrumpf and Kaiser, 2015). In the mineral soil, an increased SOC decomposition and turnover (Balesdent et al., 2018; Cécillon et al., 2018) with depth, time since bare-fallow or increase in soil temperature has been linked to a decrease in HI (Barré et al., 2016; Sebag et al., 2016; Soucémarianadin et al., 2018b; Poeplau et al., 2019). Similarly to SOC, it would be expected that POM with lower HI is less energy-rich and would require more energy to further break down (Barré et al., 2016), resulting in a greater thermal and biogeochemical stability.

However, our results suggest that differences in lability between topsoil and subsoil POM are less important in eutric Cambisols (a similar pattern was observed for total SOC;

508 Soucémarianadin et al. 2018b) and under deciduous vegetation. The chemical (higher
509 aliphatic and carbonyl + carboxyl ratios; lower aromatic ratio) and thermal (higher $T_{50\_CO2\_PYR}$
510 and HI; lower $OI_{RE6}$) characteristics of the POM from soils in deciduous dominant plots
511 suggest that it is less labile than the POM fraction from soils in coniferous plots, despite a
512 lower lignin content. Our results also suggest that POM of deciduous and coniferous plots are
513 not as different in eutric Cambisols. Compared with the POM fraction in dystric Cambisols or
514 entic Podzols, POM in eutric Cambisols presented chemical (lower C/N ratio and aliphatic
515 and carbonyl + carboxyl ratios) and thermal (lower $T_{50\_CO2\_PYR}$ and HI; higher $OI_{RE6}$)
516 properties suggesting that it was more decomposed, yet less thermally stable. These
517 differences were mostly observed in the deep layer. It could also be that the proportion of
518 pyrogenic carbon in the deep layers of eutric Cambisols is less important than in the two other
519 soil classes: as more pyrogenic carbon gets potentially stabilized in organo-mineral
520 interactions stimulated by the finer texture of the eutric Cambisols, this results in a reduced
521 vertical transfer in the soil profile for the latter soil class.
522 POM is considered as part of labile SOC (Wander, 2004) and HI, $OI_{RE6}$ and $T_{50\_CO2\_PYR}$
523 values of the POM fraction, when compared with values obtained for the bulk soil or the
524 mineral-associated OM fraction (Saenger et al., 2015; Soucémarianadin et al., 2018b),
525 reflected a lower thermal stability of the POM fraction. This lower thermal stability can be
526 linked to the shorter persistence of the fraction of total SOC present as POM in the ecosystem.
527 For instance, Baisden et al. (2002) showed that at least 90% of the free POM from topsoils of
528 Californian grasslands (with secondary oaks) was turning over in less than 10 years. In a
529 German beech forest, Schrumpf and Kaiser (2015) found a similar turnover for the free POM
530 (light fraction) in the 0–5 cm layer.
531 The potential contribution of recalcitrant pyrogenic carbon to the POM fraction should also be
532 taken into consideration as an additional source of POM heterogeneity. The presence of this

residue of the incomplete combustion of organic matter would create a strong heterogeneity in the chemical composition of the POM fraction. As pyrogenic carbon has a greater intrinsic recalcitrance due to higher condensation, which makes it less prone to decomposition (Schmidt et al., 2011), its presence could also affect POM thermal stability and overall dynamics. Hence, POM containing pyrogenic carbon would present lower $OI_{RE6}$ and HI values and increased thermal stability (*e.g.*, higher $T_{50\_CO2\_PYR}$) as shown by Poot et al. (2009) for various pyrogenic carbon samples.

Taken together, our results suggest that caution should be applied when using POM quantity as an indicator of SOC lability as the quality of the POM, hence its lability, will be strongly dependent on the ecosystem (soil type, vegetation) and depth considered.

## 5. Conclusions

The variable thermal stability of POM illustrates its heterogeneity as a labile SOC component and suggests variations in turnover of C in POM. Our results also suggested that various sources of POM inputs exist within a soil profile. Although the C in POM only corresponds to 10 to 20% of total SOC in our French forest soils, it is likely to significantly influence SOC persistence overall. While confirming that POM is part of the more labile SOC, our results showed that, in French temperate forests, depth, soil class and vegetation type were all important factors to explain the heterogeneity of POM chemistry and thermal stability. This suggests contrasting persistence of POM in soils as a function of these three factors.

## Acknowledgements

This work was supported by the French Environment & Energy Management Agency (ADEME) [APR REACCTIF, piCaSo project], Campus France [PRESTIGE-2015-3-0008] and the SOCUTE project funded by the "Emergences" program from Ville de Paris. We thank M. Bryant, S. Cecchini, J. Mériguet, F. Savignac, and L. LeVagueresse for their technical support. We acknowledge two anonymous reviewers for their time and effort in commenting on the manuscript.

## References

Aber, J.D. and Melillo, J.M., 1980. Litter decomposition: measuring relative contributions of organic matter and nitrogen to forest soils. Can. J. Bot., 58:416-421, doi:10.1139/b80-046.

Albrecht, R., Sebag, D. and Verrecchia, E., 2015. Organic matter decomposition: bridging the gap between Rock-Eval pyrolysis and chemical characterization (CPMAS $^{13}$C NMR). Biogeochemistry, 122:101-111, doi:10.1007/s10533-014-0033-8.

Amundson, R., 2001. The Carbon Budget in Soils. Annu. Rev. Earth Planet. Sci., 29:535-562, doi:10.1146/annurev.earth.29.1.535.

Angst, G., Kögel-Knabner, I., Kirfel, K., Hertel, D. and Mueller, C.W., 2016. Spatial distribution and chemical composition of soil organic matter fractions in rhizosphere and non-rhizosphere soil under European beech (Fagus sylvatica L.). Geoderma, 264:179-187, doi:10.1016/j.geoderma.2015.10.016.

Angst, G., Messinger, J., Greiner, M., Häusler, W., Hertel, D., Kirfel, K., Kögel-Knabner, I., Leuschner, C., Rethemeyer, J. and Mueller, C.W., 2018. Soil organic carbon stocks in topsoil and subsoil controlled by parent material, carbon input in the rhizosphere, and microbial-derived compounds. Soil Biol. Biochem., 122:19-30, doi:10.1016/j.soilbio.2018.03.026.

Baisden, W.T., Amundson, R., Cook, A.C. and Brenner, D.L., 2002. Turnover and storage of C and N in five density fractions from California annual grassland surface soils. Global Biogeochem. Cycles, 16:64-61; 64-16, doi:10.1029/2001GB001822.

Baldock, J.A., Oades, J.M., Nelson, P.N., Skene, T.M., Golchin, A. and Clarke, P., 1997. Assessing the extent of decomposition of natural organic materials using solid-state $^{13}C$ NMR spectroscopy. Aust. J. Soil Res., 35:1061-1084, doi:10.1071/S97004.

Baldock, J.A., Oades, J.M., Waters, A.G., Peng, X., Vassallo, A.M. and Wilson, M.A., 1992. Aspects of the chemical structure of soil organic materials as revealed by solid-state $^{13}C$ NMR spectroscopy. Biogeochemistry, 16:1-42, doi:10.1007/BF02402261.

Balesdent, J., 1996. The significance of organic separates to carbon dynamics and its modelling in some cultivated soils. Eur. J. Soil Sci., 47:485-493, doi:10.1111/j.1365-2389.1996.tb01848.x.

Balesdent, J., Basile-Doelsch, I., Chadoeuf, J., Cornu, S., Derrien, D., Fekiacova, Z. and Hatté, C., 2018. Atmosphere-soil carbon transfer as a function of soil depth. Nature, 559:599-602, doi:10.1038/s41586-018-0328-3.

Balesdent, J., Besnard, E., Arrouays, D. and Chenu, C., 1998. The dynamics of carbon in particle-size fractions of soil in a forest-cultivation sequence. Plant Soil, 201:49-57, doi:10.1023/A:1004337314970.

Balesdent, J., Pétraud, J.P. and Feller, C., 1991. Effets des ultrasons sur la distribution granulométrique des matières organiques des sols. Sci. Sol, 29:95-106.

Barré, P., Plante, A.F., Cécillon, L., Lutfalla, S., Baudin, F., Christensen, B.T., Eglin, T., Fernandez, J.M., Houot, S., Kätterer, T., Le Guillou, C., Macdonald, A., van Oort, F. and Chenu, C., 2016. The energetic and chemical signatures of persistent soil organic matter. Biogeochemistry, 130:1-12, doi:10.1007/s10533-016-0246-0.

Bates, D., Mächler, M., Bolker, B. and Walker, S., 2015. Fitting Linear Mixed-Effects Models Using lme4. Journal of Statistical Software, Articles, 67:1-48, doi:10.18637/jss.v067.i01.

Behar, F., Beaumont, V. and Penteado, D.B., 2001. Rock-Eval 6 Technology: Performances and Developments. Oil Gas Sci. Technol., 56:111-134, doi:10.2516/ogst:2001013.

Beleites, C. and Sergo, V., 2015. hyperSpec: A Package to Handle Hyperspectral Data Sets in R.

Berg, B., Liu, C., Laskowski, R. and Davey, M., 2013. Relationships between nitrogen, acid-unhydrolyzable residue, and climate among tree foliar litters. Can. J. For. Res., 43:103-107, doi:10.1139/cjfr-2012-0385.

Berg, B. and McClaugherty, C., 2013. Plant Litter: Decomposition, Humus Formation, Carbon Sequestration. Springer, Berlin, Germany.

Borchers, H.W., 2015. pracma: Practical numerical math functions.

Brêthes, A., Ulrich, E. and Lanier, M., 1997. RENECOFOR : Caractéristiques Pédologiques Des 102 Peuplements Du Réseau : Observations De 1994/95. Office national des forêts, Département des recherches techniques, Fontainebleau, France.

Carrie, J., Sanei, H. and Stern, G., 2012. Standardisation of Rock–Eval pyrolysis for the analysis of recent sediments and soils. Org. Geochem., 46:38-53, doi:10.1016/j.orggeochem.2012.01.011.

Carter, M.R., Gregorich, E.G., Angers, D.A., Donald, R.G. and Bolinder, M.A., 1998. Organic C and N storage, and organic C fractions, in adjacent cultivated and forested soils of eastern Canada. Soil Tillage Res., 47:253-261, doi:10.1016/S0167-1987(98)00114-7.

Cécillon, L., Baudin, F., Chenu, C., Houot, S., Jolivet, R., Kätterer, T., Lutfalla, S., Macdonald, A., van Oort, F., Plante, A.F., Savignac, F., Soucémarianadin, L. and Barré, P., 2018. A model based on Rock-Eval thermal analysis to quantify the size of the centennially

629 persistent organic carbon pool in temperate soils. Biogeosciences, 15: 2835-2849,
630 doi:10.5194/bg-15-2835-2018.
631 Cécillon, L., Certini, G., Lange, H., Forte, C. and Strand, L.T., 2012. Spectral fingerprinting
632 of soil organic matter composition. Org. Geochem., 46:127-136,
633 doi:10.1016/j.orggeochem.2012.02.006.
634 Christensen, B.T., 1992. Physical Fractionation of Soil and Organic Matter in Primary
635 Particle Size and Density Separates. In: B.A. Stewart (Editor). Advances in Soil Science.
636 Springer New York, New York, NY, pp. 1-90.
637 Cole, D.W. and Rapp, M., 1981. Elemental cycling in forest ecosystems. In: D.E. Reichle
638 (Editor). Dynamic Properties of Forest Ecosystems. Cambridge University Press, pp. 341-409.
639 Cools, N., Vesterdal, L., De Vos, B., Vanguelova, E. and Hansen, K., 2014. Tree species is
640 the major factor explaining C:N ratios in European forest soils. Forest Ecol. Manag., 311:3-
641 16, doi:10.1016/j.foreco.2013.06.047.
642 Cotrufo, F.M., Ineson, P. and Roberts, D.J., 1995. Decomposition of birch leaf litters with
643 varying C-to-N ratios. Soil Biol. Biochem., 27:1219-1221, doi:10.1016/0038-0717(95)00043-
644 E ".
645 Disnar, J.-R., Guillet, B., Keravis, D., Di-Giovanni, C. and Sebag, D., 2003. Soil organic
646 matter (SOM) characterization by Rock-Eval pyrolysis: scope and limitations. Org.
647 Geochem., 34:327-343, doi:10.1016/S0146-6380(02)00239-5.
648 Fissore, C., Jurgensen, M.F., Pickens, J., Miller, C., Page-Dumroese, D. and Giardina, C.P.,
649 2016. Role of soil texture, clay mineralogy, location, and temperature in coarse wood
650 decomposition—a mesocosm experiment. Ecosphere, 7:e01605, doi:10.1002/ecs2.1605.
651 Fox, J. and Weisberg, S., 2011. An R Companion to Applied Regression.

652 Golchin, A., Oades, J.M., Skjemstad, J.O. and Clarke, P., 1994. Study of free and occluded
653 particulate organic matter in soils by solid state $^{13}C$ CP/MAS NMR spectroscopy and
654 scanning electron microscopy. Aust. J. Soil Res., 32:285-309, doi:10.1071/SR9940285.
655 Gregorich, E.G., Gillespie, A.W., Beare, M.H., Curtin, D., Sanei, H. and Yanni, S.F., 2015.
656 Evaluating biodegradability of soil organic matter by its thermal stability and chemical
657 composition. Soil Biol. Biochem., 91:182-191, doi:10.1016/j.soilbio.2015.08.032.
658 Gregorich, E.G. and Janzen, H.H., 1996. Storage of Soil Carbon in the Light Fraction and
659 Macro-Organic Matter. In: M.R. Carter and B.A. Stewart (Editors). Structure and Soil
660 Organic Matter Storage in Agricultural Soils. CRC Press, Boca Raton, FL, USA, pp. 167-190.
661 Haynes, R.J., 2005. Labile organic matter fractions as central components of the quality of
662 agricultural soils: an overview. Adv. Agron. 85, 221–268, doi.org/10.1016/S0065-
663 2113(04)85005-3.
664 Hetényi, M., Nyilas, T., Sajgó, C. and Brukner-Wein, A., 2006. Heterogeneous organic
665 matter from the surface horizon of a temperate zone marsh. Org. Geochem., 37:1931-1942,
666 doi:10.1016/j.orggeochem.2006.07.019.
667 Hetényi, M., Nyilas, T. and Tóth, T.M., 2005. Stepwise Rock-Eval pyrolysis as a tool for
668 typing heterogeneous organic matter in soils. J. Anal. Appl. Pyrolysis, 74:45-54,
669 doi:10.1016/j.jaap.2004.11.012.
670 Hobbie, S.E., Oleksyn, J., Eissenstat, D.M. and Reich, P.B., 2010. Fine root decomposition
671 rates do not mirror those of leaf litter among temperate tree species. Oecologia, 162:505-513,
672 doi:10.1007/s00442-009-1479-6.
673 IUSS Working Group, 2015. World reference base for soil resources 2014 (update 2015),
674 international soil classification system for naming soils and creating legends for soil maps.
675 World Soil Resources Reports.

Jackson, R.B., Mooney, H.A. and Schulze, E., 1997. A global budget for fine root biomass, surface area, and nutrient contents. PNAS, 94:7362-7366, doi:10.1073/pnas.94.14.7362.

Jonard, M., Nicolas, M., Coomes, D.A., Caignet, I., Saenger, A. and Ponette, Q., 2017. Forest soils in France are sequestering substantial amounts of carbon. Sci. Total Environ., 574:616-628, doi:10.1016/j.scitotenv.2016.09.028.

Kögel-Knabner, I., 2002. The macromolecular organic composition of plant and microbial residues as inputs to soil organic matter. Soil Biol. Biochem., 34:139-162, doi:10.1016/S0038-0717(01)00158-4.

Kölbl, A. and Kögel-Knabner, I., 2004. Content and composition of free and occluded particulate organic matter in a differently textured arable Cambisol as revealed by solid-state $^{13}C$ NMR spectroscopy. Z. Pflanzenernähr. Bodenk., 167:45-53, doi:10.1002/jpln.200321185.

Laganière, J., Angers, D.A., Paré, D., Bergeron, Y. and Chen, H.Y.H., 2011. Black spruce soils accumulate more uncomplexed organic matter than aspen soils. Soil Sci Soc Am J, 75:1125-1132, doi:10.2136/sssaj2010.0275.

Leifeld, J., Zimmerman, M., Fuhrer, J. and Conen, F., 2009. Storage and turnover of carbon in grassland soils along an elevation gradient in the Swiss Alps. Global Change Biol., 15:668-679, doi:10.1111/j.1365-2486.2008.01782.x.

Melillo, J.M., Aber, J.D. and Muratore, J.F., 1982. Nitrogen and lignin control of hardwood leaf litter decomposition dynamics. Ecology, 63:621-626, doi:10.2307/1936780.

Natelhoffer, K.J. and Fry, B., 1988. Controls on natural nitrogen-15 and carbon-13 abundances in forest soil organic matter. 52:1633-1640, doi:10.2136/sssaj1988.03615995005200060024x.

Ng, E., Patti, A.F., Rose, M.T., Schefe, C.R., Wilkinson, K., Smernik, R.J. and Cavagnaro, T.R., 2014. Does the chemical nature of soil carbon drive the structure and functioning of soil microbial communities? Soil Biol. Biochem., 70:54-61, doi:10.1016/j.soilbio.2013.12.004.

Nguyen, T.T., Janik, L.J. and Raupach, M., 1991. Diffuse reflectance infrared fourier transform (DRIFT) spectroscopy in soil studies. Aust. J. Soil Res., 29:49-67, doi:10.1071/SR9910049.

Oades, J.M., 1972. Studies on soil polysaccharides. III. Composition of polysaccharides in some Australian soils. Soil Res., 10:113-126, doi:10.1071/SR9720113.

Oades, J.M., Vassallo, A.M., Waters, A.G. and Wilson, M.A., 1987. Characterization of organic matter in particle size and density fractions from a red-brown earth by solid state $^{13}C$ NMR. Aust. J. Soil Res., 25:71-82, doi:10.1071/SR9870071.

Pengerud, A., Cécillon, L., Johnsen, L.K., Rasse, D.P. and Strand, L.T., 2013. Permafrost Distribution Drives Soil Organic Matter Stability in a Subarctic Palsa Peatland. Ecosystems, 16:934-947, doi:10.1007/s10021-013-9652-5.

Pinheiro, J., Bates, D., DebRoy, S., Sarkar, D. and Team, R.C., 2016. Nlme: Linear and Nonlinear Mixed Effects Models.

Poeplau, C., Barré, P., Cécillon, L., Baudin, F. and Sigurdsson, B.D., 2019. Changes in the Rock-Eval signature of soil organic carbon upon extreme soil warming and chemical oxidation - A comparison. Geoderma, 337:181-190, doi:10.1016/j.geoderma.2018.09.025.

Poeplau, C. and Don, A., 2013. Sensitivity of soil organic carbon stocks and fractions to different land-use changes across Europe. Geoderma, 192:189-201, doi:10.1016/j.geoderma.2012.08.003.

Ponette, Q., Ulrich, E., Brêthes, A., Bonneau, M. and Lanier, M., 1997. RENECOFOR - Chimie Des Sols Dans Les 102 Peuplements Du Réseau : Campagne De Mesures 1993-95. ONF, Département des recherches techniques, Fontainebleau, France.

Poot, A., Quik, J.T.K., Veld, H. and Koelmans, A.A., 2009. Quantification methods of Black Carbon: Comparison of Rock-Eval analysis with traditional methods. Journal of Chromatography A, 1216:613-622, doi:10.1016/j.chroma.2008.08.011.

726 Prescott, C.E., 2010. Litter decomposition: what controls it and how can we alter it to
727 sequester more carbon in forest soils? Biogeochemistry, 101:133-149, doi:10.1007/s10533-
728 010-9439-0.
729 Preston, C.M., Trofymow, J.A. and the Canadian Intersite Decomposition Experiment
730 Working Group, 2000. Variability in litter quality and its relationship to litter decay in
731 Canadian forests. Can. J. Bot., 78:1269-1287, doi:10.1139/b00-101.
732 Puissant, J., Mills, R.T.E., Robroek, B.J.M., Gavazov, K., Perrette, Y., De Danieli, S.,
733 Spiegelberger, T., Buttler, A., Brun, J. and Cécillon, L., 2017. Climate change effects on the
734 stability and chemistry of soil organic carbon pools in a subalpine grassland.
735 Biogeochemistry, 132:123-139, doi:10.1007/s10533-016-0291-8.
736 Quideau, S.A., Chadwick, O.A., Benesi, A., Graham, R.C. and Anderson, M.A., 2001. A
737 direct link between forest vegetation type and soil organic matter composition. Geoderma,
738 104:41-60, doi:10.1016/S0016-7061(01)00055-6.
739 R Core Team, 2016. R: A Language and Environment for Statistical Computing.
740 Rasse, D., Rumpel, C. and Dignac, M., 2005. Is soil carbon mostly root carbon?
741 Mechanisms for a specific stabilisation. Plant Soil, 269:341-356, doi:10.1007/s11104-004-
742 0907-y.
743 Reeves, J.B., 2012. Mid-infrared spectral interpretation of soils: Is it practical or accurate?
744 Geoderma, 189-190:508-513, doi:10.1016/j.geoderma.2012.06.008.
745 Robroek, B.J.M., Jassey, V.E.J., Kox, M.A.R., Berendsen, R.L., Mills, R.T.E., Cécillon, L.,
746 Puissant, J., Meima-Franke, M., Bakker, P.A.H.M. and Bodelier, P.L.E., 2015. Peatland
747 vascular plant functional types affect methane dynamics by altering microbial community
748 structure. J. Ecol., 103:925-934, doi:10.1111/1365-2745.12413.
749 Rowley, M.C., Grand, S. and Verrecchia, E.P., 2018. Calcium-mediated stabilisation of soil
750 organic carbon. Biogeochemistry, 137:27-49, doi:10.1007/s10533-017-0410-1.

751 Rumpel, C., Kögel-Knabner, I. and Bruhn, F., 2002. Vertical distribution, age, and chemical
752 composition of organic carbon in two forest soils of different pedogenesis. Org. Geochem.,
753 33:1131-1142, doi:10.1016/S0146-6380(02)00088-8.
754 Saenger, A., Cécillon, L., Poulenard, J., Bureau, F., De Daniéli, S., Gonzalez, J. and Brun,
755 J., 2015. Surveying the carbon pools of mountain soils: A comparison of physical
756 fractionation and Rock-Eval pyrolysis. Geoderma, 241–242:279-288,
757 doi:10.1016/j.geoderma.2014.12.001.
758 Sarkhot, D.V., Comerford, N.B., Jokela, E.J., Reeves, J.B. and Harris, W.G., 2007.
759 Aggregation and aggregate carbon in a forested Southeastern coastal plain Spodosol. Soil Sci.
760 Soc. Am. J., 71:1779-1787, doi:10.2136/sssaj2006.0340.
761 Schmidt, M.W.I., Torn, M.S., Abiven, S., Dittmar, T., Guggenberger, G., Janssens, I.A.,
762 Kleber, M., Kögel-Knabner, I., Lehmann, J., Manning, D.A.C., Nannipieri, P., Rasse, D.P.,
763 Weiner, S. and Trumbore, S.E., 2011. Persistence of soil organic matter as an ecosystem
764 property. Nature, 478:49-56, doi:10.1038/nature10386.
765 Schrumpf, M. and Kaiser, K., 2015. Large differences in estimates of soil organic carbon
766 turnover in density fractions by using single and repeated radiocarbon inventories. Geoderma,
767 239–240:168-178, doi:10.1016/j.geoderma.2014.09.025.
768 Schrumpf, M., Kaiser, K., Guggenberger, G., Persson, T., Kögel-Knabner, I. and Schulze,
769 E., 2013. Storage and stability of organic carbon in soils as related to depth, occlusion within
770 aggregates, and attachment to minerals. Biogeosciences, 10:1675-1691, doi:10.5194/bg-10-
771 1675-2013.
772 Sebag, D., Disnar, J.-R., Guillet, B., Di Giovanni, C., Verrecchia, E.P. and Durand, A.,
773 2006. Monitoring organic matter dynamics in soil profiles by 'Rock-Eval pyrolysis': bulk
774 characterization and quantification of degradation. Eur. J. Soil Sci., 57:344-355,
775 doi:10.1111/j.1365-2389.2005.00745.x.

776 Sebag, D., Verrecchia, E.P., Cécillon, L., Adatte, T., Albrecht, R., Aubert, M., Bureau, F.,
777 Cailleau, G., Copard, Y., Decaens, T., Disnar, J.-R., Hetényi, M., Nyilas, T. and Trombino,
778 L., 2016. Dynamics of soil organic matter based on new Rock-Eval indices. Geoderma,
779 284:185-203, doi:10.1016/j.geoderma.2016.08.025.
780 Soucémarianadin, L.N., Cécillon, L., Chenu, C., Baudin, F., Nicolas, M., Girardin, C. and
781 Barré, P., 2018a. Is Rock-Eval 6 thermal analysis a good indicator of soil organic carbon
782 lability? - A method-comparison study in forest soils. Soil Biol. Biochem., 117:108-116,
783 doi:10.1016/j.soilbio.2017.10.025.
784 Soucémarianadin, L.N., Cécillon, L., Guenet, B., Chenu, C., Baudin, F., Nicolas, M.,
785 Girardin, C. and Barré, P., 2018b. Environmental factors controlling soil organic carbon
786 stability in French forest soils. Plant Soil, 426:267-286, doi:10.1007/s11104-018-3613-x.
787 Spycher, G., Sollins, P. and Rose, S., 1983. Carbon and nitrogen in the light fraction of a
788 forest soil: vertical distribution and seasonal patterns. Soil Sci., 135:79-87,
789 doi:10.1097/00010694-198302000-00002.
790 Swift, M.J., Heal, O.W. and Anderson, J.M., 1979. Decomposition in Terrestrial
791 Ecosystems. Blackwell, Oxford.
792 Trumbore, S.E., 1997. Potential responses of soil organic carbon to global environmental
793 change. Proc. Natl. Acad. Sci. U. S. A., 94:8284-8291.
794 Trumbore, S.E., Chadwick, O.A. and Amundson, R., 1996. Rapid exchange between soil
795 carbon and atmospheric carbon dioxide driven by temperature change. Science, 272:393-396,
796 doi:10.1126/science.272.5260.393.
797 Ulrich, E., 1995. Le réseau RENECOFOR : objectifs et réalisation. Rev. for. fr., 47:107-124,
798 doi:10.4267/2042/26634.

Wander, M., 2004. Soil organic matter fractions and their relevance to soil function. In: F. Magdoff and R.R. Weil (Editors). Soil Organic Matter in Sustainable Agriculture. CRC Press, pp. 67-102.

Whitehead, D.C., Buchan, H. and Hartley, R.D., 1975. Components of soil organic matter under grass and arable cropping. Soil Biol. Biochem., 7:65-71, doi:10.1016/0038-0717(75)90033-4.

Yeasmin, S., Singh, B., Johnston, C.T. and Sparks, D.L., 2017. Organic carbon characteristics in density fractions of soils with contrasting mineralogies. Geochim. Cosmochim. Acta, 218:215-236, doi:10.1016/j.gca.2017.09.007.

Zhang, J., Song, C. and Wenyan, Y., 2007. Tillage effects on soil carbon fractions in the Sanjiang Plain, Northeast China. Soil Tillage Res., 93:102-108, doi:10.1016/j.still.2006.03.014.

## Figures captions

**Fig. 1.** (a) Location of the 52 study sites from the French national network for the long term monitoring of forest ecosystems (RENECOFOR) and their repartition among the vegetation types and soil classes; (b) Number of samples by depths and analyses performed to characterize the POM.

**Fig. 2.** Interactions depth × soil class for C/N ratio, $T_{50\_CO2\_PYR}$ and MIR-ATR derived aliphatic ratio and aromatic ratio. The horizontal black line shows the median. The bottom and top of the box show the first and third quartiles, respectively. Different letters indicate significant differences among the three soil classes in topsoil or subsoil for each parameter.

**Fig. 3.** Interactions depth × vegetation type for the MIR-ATR derived carbonyl + carboxyl ratio and the RE6 Hydrogen Index (corrected) and $T_{50\_CO2\_PYR}$. The horizontal black line shows the median. The bottom and top of the box show the first and third quartiles, respectively. Different letters indicate significant differences between vegetation types in topsoil or subsoil for each parameter.

# Tables

**Table 1**. Details of models and their significant terms selected to explain variations in parameters from Rock-Eval 6 (HI corrected, $OI_{RE6}$, and $T_{50\_CO2\_PYR}$) and elemental analysis (C/N ratio) and ratios derived from MIR-ATR spectroscopy (aliphatic, ether and alcohol, aromatic, carbonyl and carboxyl) for the POM fraction of the 52 study plots. All models used a gls function (see details in the *Calculations and statistical analyses* section § 2.6). Significance is indicated as follows: ***: $p < 0.001$; **: $p < 0.01$; *: $p < 0.05$. The number of samples considered in each model is provided; outliers were determined with Cook's distance.

| Response variable | Transformation | Predictors in final model[a] and level of significance | n |
|---|---|---|---|
| HI corrected (HI) | sqrt (HI) | depth*** + soil*** + veg*** + depth × veg*** | 86 |
| $OI_{RE6}$ | $\log_{10}$ ($OI_{RE6}$) | soil*** + veg*** + soil × veg** | 86 |
| $T_{50\_CO2\_PYR}$ | | depth*** + soil*** + veg*** + depth × soil*** | 84 |
| C/N ratio | $\log_{10}$ (C/N) | depth*** + soil*** + depth × soil*** | 85 |
| aliphatic ratio (ali) | 1/ali | soil*** + veg*** + depth × soil** | 84 |
| aromatic ratio (arom) | 1/arom | depth*** + veg*** + depth × soil** + soil × veg*** | 84 |
| ether + alcohol ratio (ether) | 1/ether | depth*** | 84 |
| carbonyl + carboxyl ratio (carbo) | sqrt (carbo) | depth*** + soil*** + veg*** + depth × veg** + soil × veg** | 85 |

[a] For all models, we used the compound symmetry structure [corCompSymm(form =~ 1|plot)], which is similar to the variance structure of a random-intercept-only model. In our case, it allowed to treat each site as random factor.

**Table 2.** Mean, standard deviation (sd), minimum (min) and maximum (max) values of the parameters derived from elemental analysis and Rock-Eval thermal analysis as well as the ratios of C functions derived from MIR-ATR spectroscopy for the POM fraction for each depth, soil class and vegetation type. For each parameter, different letters indicate significant differences among means of the classes of the three factors (depth, soil class and vegetation type). Differences were observed for transformed data as specified in Table 1.

| | **C/N ratio** | | | | **HI corrected** (mg HC·g$^{-1}$ OC) | | | | **$OI_{RE6}$** (mg $O_2$·g$^{-1}$ TOC) | | | | **$T_{50\_CO2\_PYR}$** (°C) | | | |
|---|---|---|---|---|---|---|---|---|---|---|---|---|---|---|---|---|
| | mean | sd | min | max | mean | sd | min | max | mean | sd | min | max | mean | sd | min | max |
| **DEPTH** | | | | | | | | | | | | | | | | |
| surface | 30$^{a}$ | 8 | 20 | 71 | 301$^{a}$ | 86 | 187 | 504 | 177$^{a}$ | 29 | 107 | 247 | 351$^{a}$ | 5 | 341 | 363 |
| deep | 48$^{b}$ | 11 | 28 | 78 | 248$^{b}$ | 108 | 106 | 493 | 186$^{a}$ | 45 | 106 | 302 | 363$^{b}$ | 9 | 348 | 388 |
| **SOIL** | | | | | | | | | | | | | | | | |
| dystric Cambisol | 42$^{a}$ | 14 | 22 | 78 | 305$^{a}$ | 114 | 107 | 504 | 158$^{a}$ | 29 | 106 | 222 | 360$^{a}$ | 10 | 346 | 388 |
| eutric Cambisol | 34$^{b}$ | 7 | 22 | 50 | 244$^{b}$ | 87 | 106 | 454 | 214$^{b}$ | 30 | 154 | 302 | 351$^{b}$ | 5 | 341 | 363 |
| entic Podzol | 40$^{ab}$ | 15 | 20 | 71 | 280$^{ab}$ | 89 | 132 | 436 | 171$^{a}$ | 27 | 125 | 221 | 358$^{a}$ | 9 | 345 | 375 |
| **VEGETATION** | | | | | | | | | | | | | | | | |
| coniferous | 40$^{a}$ | 15 | 20 | 78 | 213$^{a}$ | 59 | 106 | 332 | 194$^{a}$ | 26 | 134 | 259 | 355$^{a}$ | 8 | 341 | 375 |
| deciduous | 37$^{a}$ | 11 | 22 | 71 | 346$^{b}$ | 88 | 186 | 504 | 166$^{b}$ | 42 | 106 | 302 | 358$^{b}$ | 10 | 345 | 388 |
| **ALL** | 39 | 12 | 22 | 71 | 277 | 90 | 106 | 461 | 181 | 33 | 120 | 265 | 356 | 8 | 344 | 377 |

| | **aliphatic ratio** | | | | **carbonyl + carboxyl ratio** | | | | **aromatic ratio** | | | | **ether + alcohol ratio** | | | |
|---|---|---|---|---|---|---|---|---|---|---|---|---|---|---|---|---|
| | mean | sd | min | max | mean | sd | min | max | mean | sd | min | max | mean | sd | min | max |
| **DEPTH** | | | | | | | | | | | | | | | | |
| surface | 0.186$^{a}$ | 0.014 | 0.160 | 0.223 | 0.221$^{a}$ | 0.025 | 0.164 | 0.278 | 0.236$^{a}$ | 0.038 | 0.172 | 0.329 | 0.357$^{a}$ | 0.019 | 0.330 | 0.412 |
| deep | 0.186$^{a}$ | 0.014 | 0.158 | 0.213 | 0.204$^{b}$ | 0.026 | 0.155 | 0.253 | 0.274$^{b}$ | 0.038 | 0.204 | 0.340 | 0.336$^{b}$ | 0.017 | 0.309 | 0.394 |
| **SOIL** | | | | | | | | | | | | | | | | |
| dystric Cambisol | 0.192$^{a}$ | 0.016 | 0.161 | 0.223 | 0.226$^{a}$ | 0.023 | 0.176 | 0.278 | 0.236$^{a}$ | 0.037 | 0.172 | 0.305 | 0.347$^{a}$ | 0.017 | 0.314 | 0.386 |
| eutric Cambisol | 0.178$^{b}$ | 0.010 | 0.158 | 0.201 | 0.190$^{b}$ | 0.020 | 0.155 | 0.247 | 0.285$^{a}$ | 0.040 | 0.172 | 0.340 | 0.348$^{a}$ | 0.024 | 0.314 | 0.412 |
| entic Podzol | 0.188$^{a}$ | 0.011 | 0.170 | 0.212 | 0.224$^{a}$ | 0.020 | 0.177 | 0.255 | 0.241$^{a}$ | 0.031 | 0.191 | 0.300 | 0.347$^{a}$ | 0.022 | 0.309 | 0.412 |
| **VEGETATION** | | | | | | | | | | | | | | | | |
| coniferous | 0.181$^{a}$ | 0.009 | 0.158 | 0.203 | 0.207$^{a}$ | 0.021 | 0.155 | 0.250 | 0.268$^{a}$ | 0.030 | 0.210 | 0.340 | 0.344$^{a}$ | 0.015 | 0.309 | 0.373 |
| deciduous | 0.191$^{b}$ | 0.016 | 0.160 | 0.223 | 0.220$^{b}$ | 0.031 | 0.162 | 0.278 | 0.239$^{b}$ | 0.048 | 0.172 | 0.330 | 0.350$^{a}$ | 0.025 | 0.314 | 0.412 |
| **ALL** | 0.186 | 0.013 | 0.161 | 0.214 | 0.213 | 0.024 | 0.163 | 0.262 | 0.254 | 0.038 | 0.185 | 0.326 | 0.347 | 0.020 | 0.314 | 0.400 |

# Supplementary materials

## APPENDIX A – information related to the analysis of POM chemistry and thermal stability

**Fig. A.1.** Absorbance spectra (with offset-correction) of the 86 POM samples considered in this study. The four spectral regions of interest used for the calculation of the relative aliphatic (2950–2900 $cm^{-1}$), carbonyl + carboxyl (1750–1690 $cm^{-1}$), aromatic (1605–1575 $cm^{-1}$) and ether + alcohol (1180–1145 $cm^{-1}$) ratios are indicated.

**Fig. A.2.** Description of the Rock-Eval 6 thermal analysis (adapted from Baudin et al. 2017) and calculation of the three RE6-derived parameters (Hydrogen Index; Oxygen Index and $T_{50\_CO2\_PYR}$, the temperature at which 50% of the SOM converted to $CO_2$ had evolved during the pyrolysis phase).

Reference: Baudin, F., Tribovillard, N. and Trichet, J., 2017. Géologie De La Matière Organique. 324 pp. EDP Sciences, Lille, France.

## APPENDIX B – chemical and thermal characteristics of the 86 selected samples

**Table B.1**. Values of the parameters derived from elemental analysis and Rock-Eval thermal analysis as well as the ratios of C functions derived from MIR-ATR spectroscopy for the POM fraction for each of the 86 POM samples considered in this study. For comparison, HI values without and with correction for the inorganic carbon are included.

## APPENDIX C – information related to the distribution of the 86 POM samples among the different classes of environmental factors (depth; soil class; vegetation type)

**Table C.1**. Distribution of the 86 POM samples considered in this study among the various classes of depth (surface and deep layers; 0–10 cm and 40–80 cm), soil (dystric Cambisol, eutric Cambisol, entic Podzol) and vegetation (coniferous and deciduous).

## APPENDIX D – effects of interactions of the environmental factors on POM chemistry and thermal parameters

**Fig. D.1.** Interactions soil class × vegetation type for MIR-ATR derived aromatic ratio and carbonyl + carboxyl ratio and the $OI_{RE6}$. Different letters indicate significant differences among the three soil classes in coniferous or deciduous plots for each parameter.

## APPENDIX E – correlations between parameters of POM chemistry and thermal stability

**Table E.1**. Table of correlations for all samples and for each layer individually between the POM chemical properties (C/N ratio, ether + alcohol ratio, aromatic ratio, carbonyl + carboxyl ratio, aliphatic ratio) and POM thermal stability (HI corrected, $OI_{RE6}$, $T_{50\_CO2\_PYR}$). Significance is indicated as follows: ***: $p < 0.001$; **: $p < 0.01$; *: $p < 0.05$. The high (> 0.6) correlations between parameters derived from different methods are marked in bold. n = 86 for all layers; n = 46 for surface layer and n = 40 for deep layer, respectively.

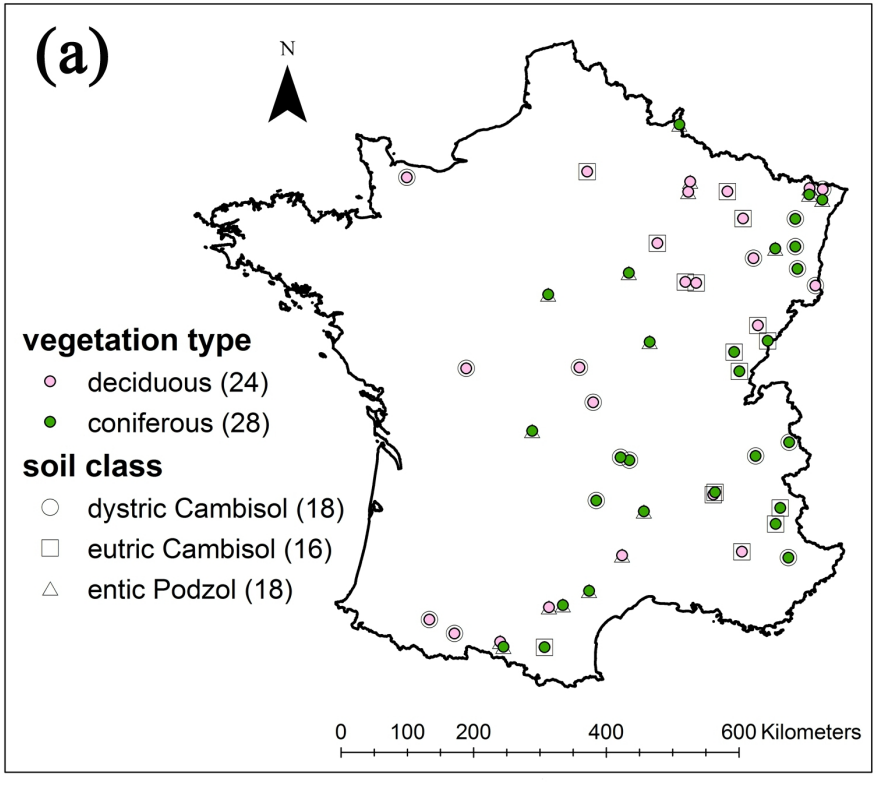
(a)
N
vegetation type
deciduous (24)
coniferous (28)
soil class
dystric Cambisol (18)
eutric Cambisol (16)
entic Podzol (18)
0 100 200 400 600 Kilometers

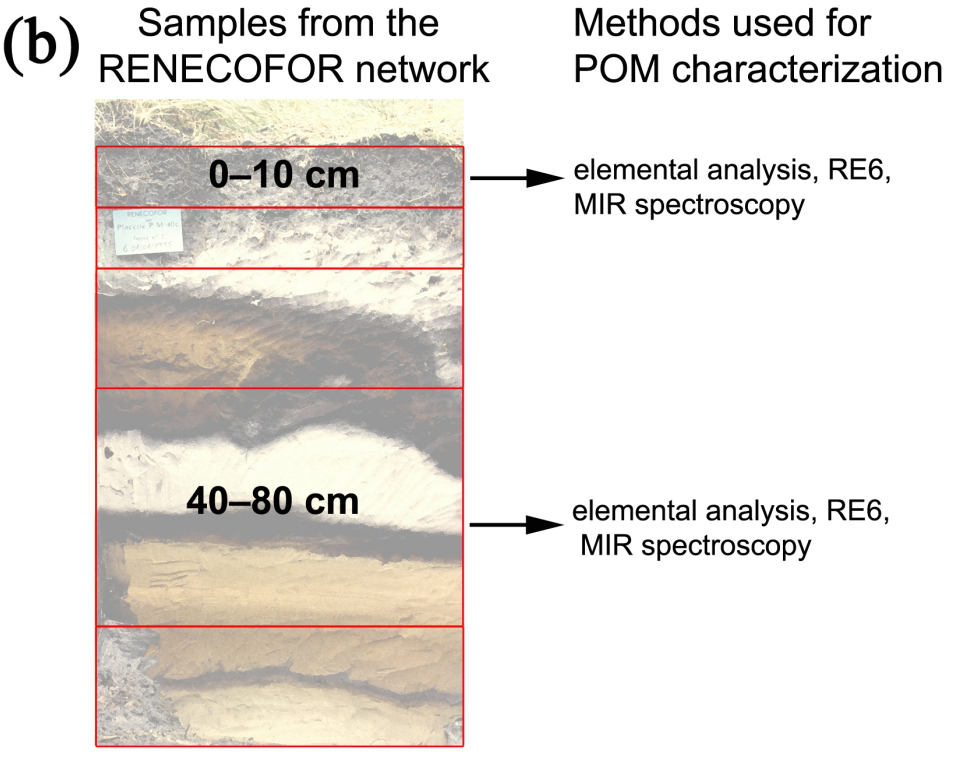
(b)
Samples from the RENECOFOR network
Methods used for POM characterization
0–10 cm
elemental analysis, RE6, MIR spectroscopy
40–80 cm
elemental analysis, RE6, MIR spectroscopy

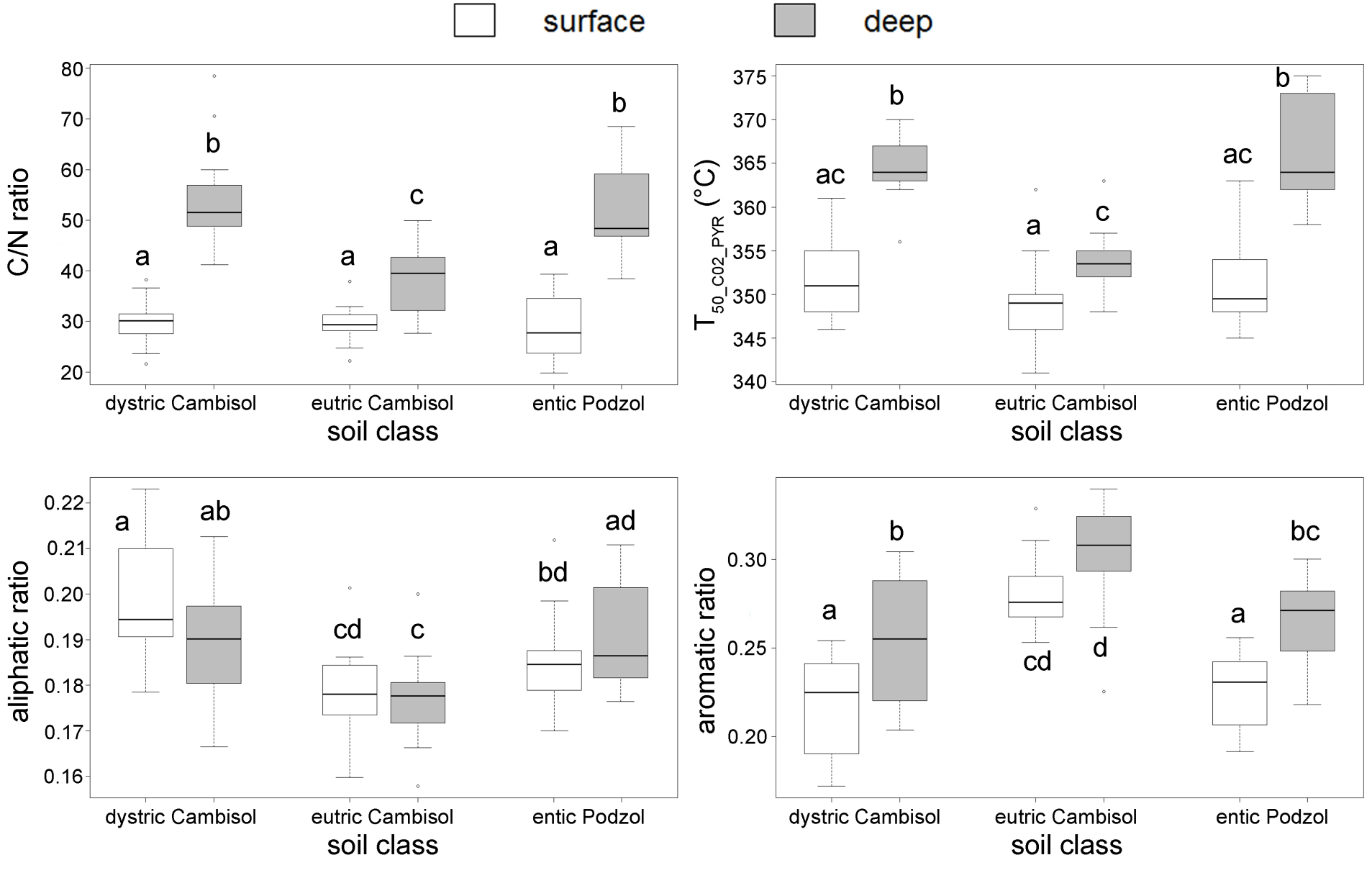
surface
deep
C/N ratio
80
70
60
50
40
30
20
a
b
a
c
a
b
dystric Cambisol
eutric Cambisol
entic Podzol
soil class
$T_{50\_C02\_PYR}$ (°C)
375
370
365
360
355
350
345
340
ac
b
a
c
ac
b
dystric Cambisol
eutric Cambisol
entic Podzol
soil class
aliphatic ratio
0.22
0.21
0.20
0.19
0.18
0.17
0.16
a
ab
cd
c
bd
ad
dystric Cambisol
eutric Cambisol
entic Podzol
soil class
aromatic ratio
0.30
0.25
0.20
a
b
cd
d
a
bc
dystric Cambisol
eutric Cambisol
entic Podzol
soil class

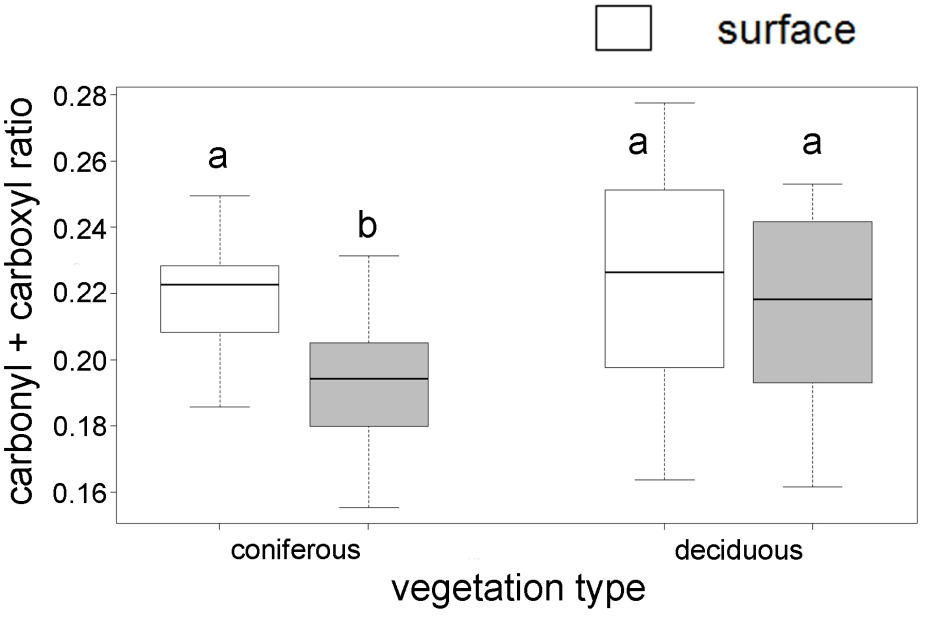
surface
carbonyl + carboxyl ratio
0.28
0.26
0.24
0.22
0.20
0.18
0.16
a
b
a
a
coniferous
deciduous
vegetation type

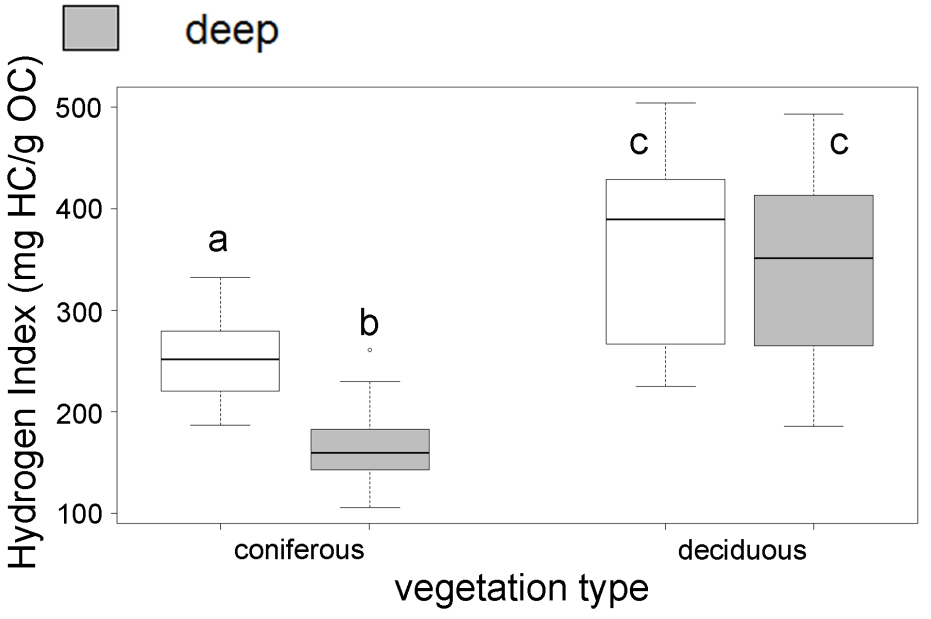
deep
Hydrogen Index (mg HC/g OC)
500
400
300
200
100
a
b
c
c
coniferous
deciduous
vegetation type

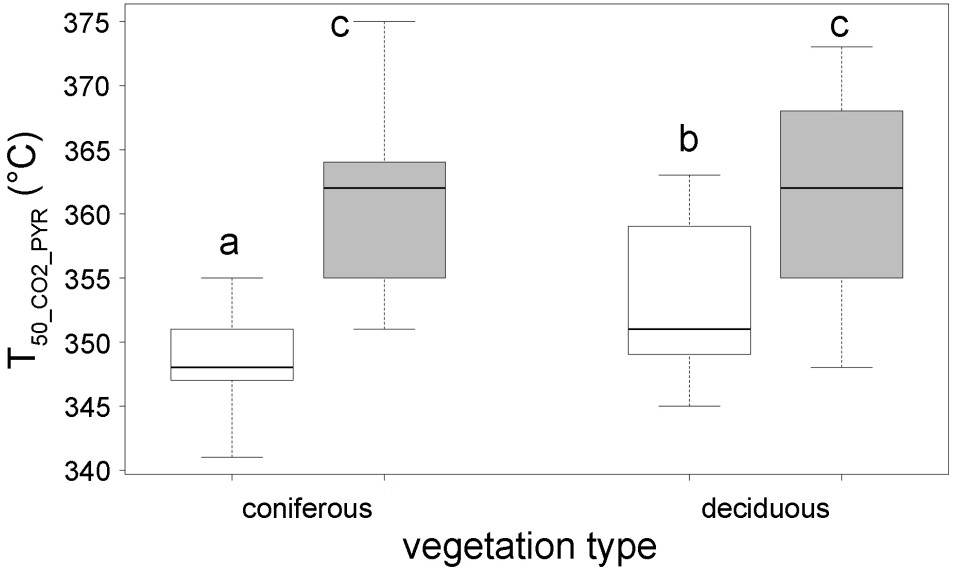
T50_CO2_PYR (°C)
375
370
365
360
355
350
345
340
a
c
b
c
coniferous
deciduous
vegetation type

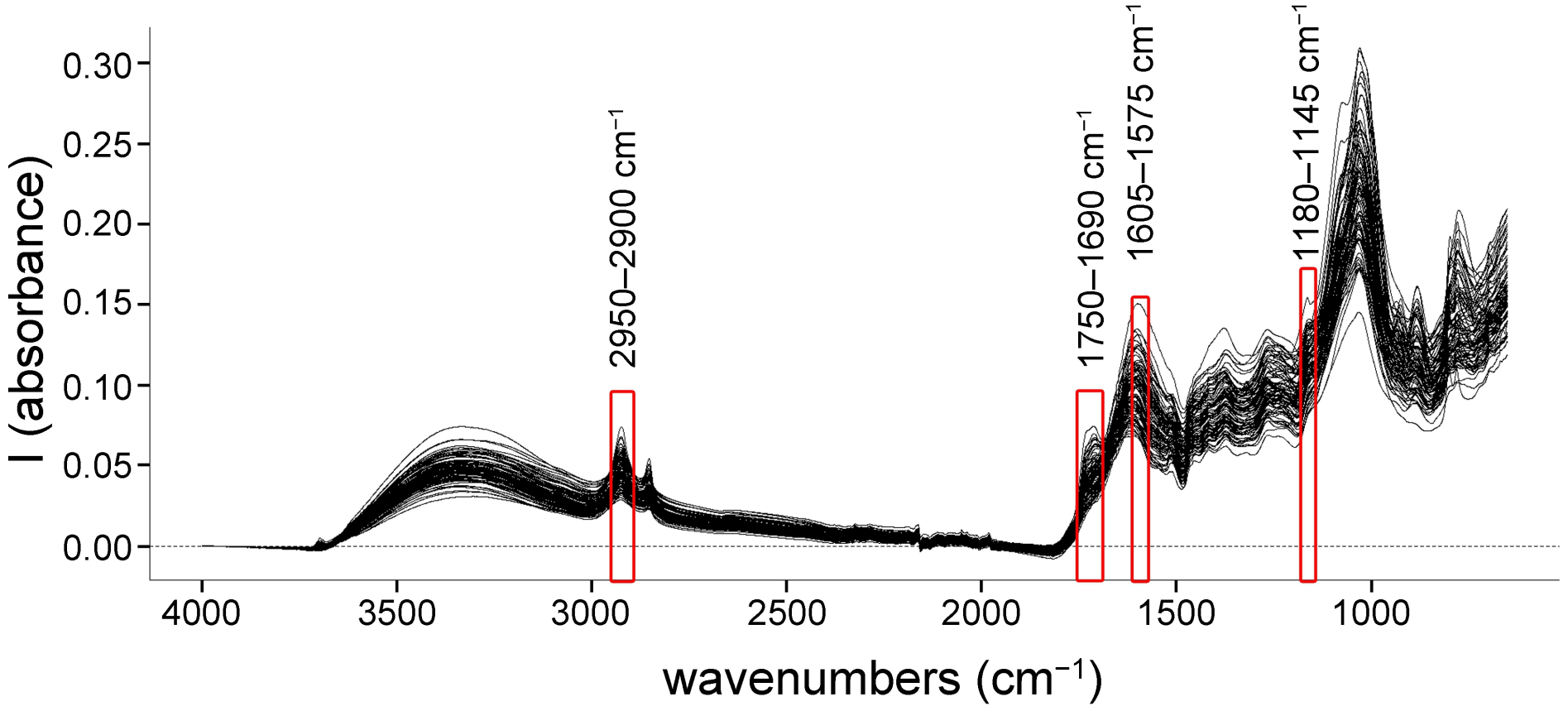
I (absorbance)
0.30
0.25
0.20
0.15
0.10
0.05
0.00
2950–2900 cm⁻¹
1750–1690 cm⁻¹
1605–1575 cm⁻¹
1180–1145 cm⁻¹
4000
3500
3000
2500
2000
1500
1000
wavenumbers (cm⁻¹)

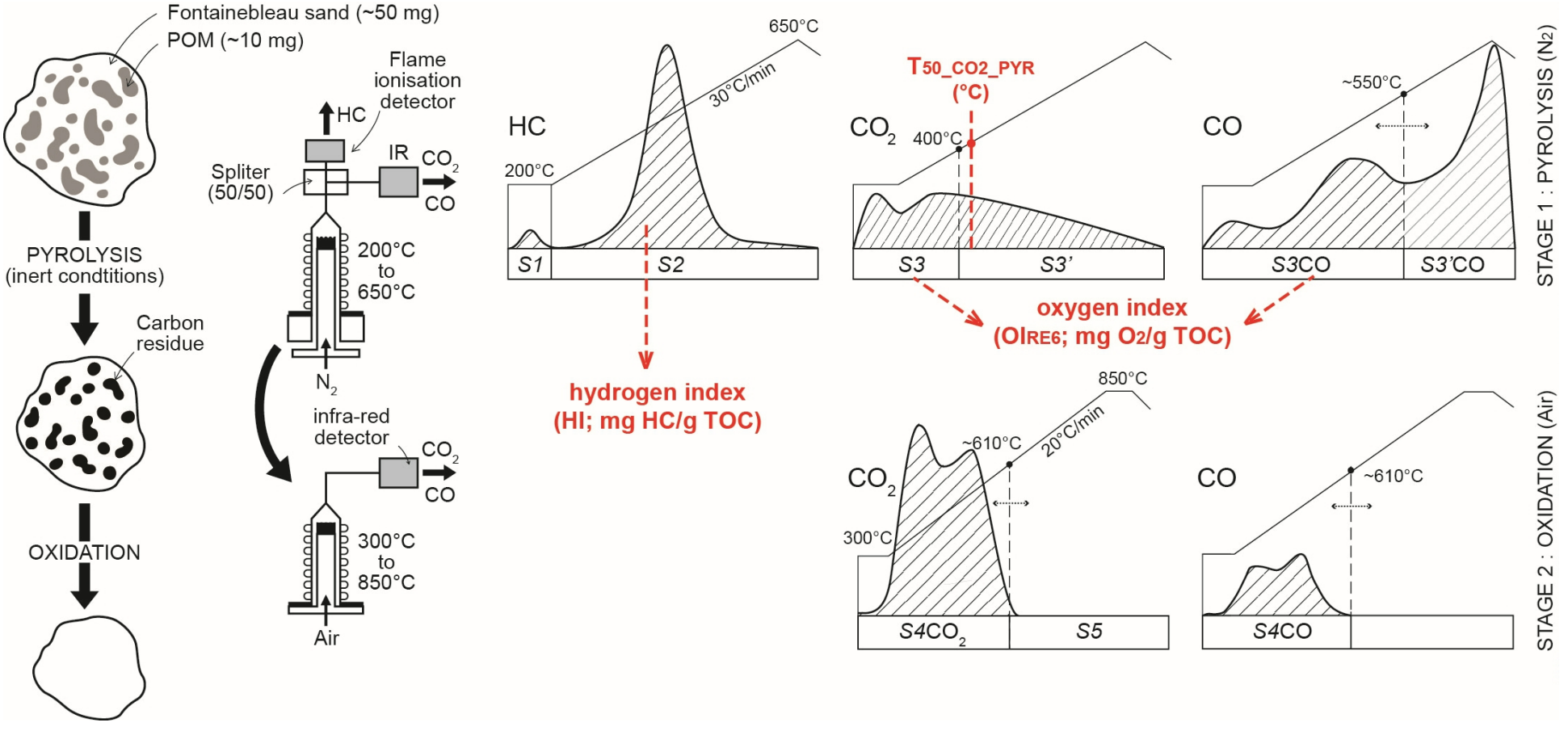
Fontainebleau sand (~50 mg)
POM (~10 mg)
PYROLYSIS
(inert condtitions)
Carbon
residue
OXIDATION
Flame
ionisation
detector
HC
IR
CO2
CO
Spliter
(50/50)
200°C
to
650°C
N2
infra-red
detector
CO2
CO
300°C
to
850°C
Air
650°C
30°C/min
HC
200°C
S1
S2
hydrogen index
(HI; mg HC/g TOC)
T50_CO2_PYR
(°C)
CO2
400°C
S3
S3'
CO
~550°C
S3CO
S3'CO
oxygen index
(OIRE6; mg O2/g TOC)
STAGE 1 : PYROLYSIS (N2)
850°C
20°C/min
~610°C
CO2
300°C
S4CO2
S5
CO
~610°C
S4CO
STAGE 2 : OXIDATION (Air)

**Table B.1.** Values of the parameters derived from elemental analysis and Rock-Eval thermal analysis as well as the ratios of C functions derived from MIR-ATR spectroscopy for the POM fraction for each of the 86 POM samples considered in this study. For comparison, HI values without and with correction for the inorganic carbon are included.

| samples | layer | vegetation type | soil class | C/N ratio | HI mg HC·g$^{-1}$ TOC) | HI corrected (mg HC·g$^{-1}$ OC) | $OI_{RE6}$ (mg $O_2$·g$^{-1}$ TOC) | $T_{50\_CO2\_PYR}$ (°C) | ether + alcohol ratio (1180–1145 cm$^{-1}$) | aromatic ratio (1605–1575 cm$^{-1}$) | carbonyl + carboxyl ratio (1690–1750 cm$^{-1}$) | aliphatic ratio (2950–2900 cm$^{-1}$) |
|---|---|---|---|---|---|---|---|---|---|---|---|---|
| CHP10_1 | surface | deciduous | eutric Cambisol | 25 | 467 | 454 | 177 | 347 | 0.412 | 0.172 | 0.232 | 0.184 |
| CHP10_4 | deep | deciduous | eutric Cambisol | 31 | 433 | 433 | 302 | 363 | 0.393 | 0.225 | 0.197 | 0.184 |
| CHP55_1 | surface | deciduous | eutric Cambisol | 32 | 450 | 436 | 166 | 349 | 0.366 | 0.186 | 0.247 | 0.201 |
| CHP55_4 | deep | deciduous | eutric Cambisol | 28 | 416 | 399 | 187 | 354 | 0.314 | 0.262 | 0.225 | 0.200 |
| CHP65_1 | surface | deciduous | dystric Cambisol | 31 | 417 | 404 | 169 | 349 | 0.381 | 0.199 | 0.226 | 0.194 |
| CHP65_4 | deep | deciduous | dystric Cambisol | 71 | 345 | 330 | 106 | 388 | 0.353 | 0.217 | 0.241 | 0.189 |
| CHS03_1 | surface | deciduous | dystric Cambisol | 29 | 471 | 446 | 134 | 350 | 0.358 | 0.181 | 0.251 | 0.210 |
| CHS03_4 | deep | deciduous | dystric Cambisol | 51 | 506 | 493 | 136 | 362 | 0.362 | 0.208 | 0.218 | 0.213 |
| CHS51_1 | surface | deciduous | entic Podzol | 28 | 401 | 363 | 148 | 349 | 0.412 | 0.192 | 0.217 | 0.179 |
| CHS57b_1 | surface | deciduous | entic Podzol | 24 | 398 | 389 | 154 | 348 | 0.383 | 0.194 | 0.225 | 0.198 |
| CHS68_1 | surface | deciduous | dystric Cambisol | 26 | 440 | 429 | 158 | 351 | 0.362 | 0.206 | 0.237 | 0.195 |
| CHS86_1 | surface | deciduous | dystric Cambisol | 31 | 259 | 251 | 138 | 360 | 0.386 | 0.230 | 0.222 | 0.161 |
| CHS86_4 | deep | deciduous | dystric Cambisol | 48 | 364 | 351 | 135 | 368 | 0.337 | 0.255 | 0.213 | 0.195 |
| CPS67_1 | surface | deciduous | dystric Cambisol | 38 | 431 | 421 | 107 | 361 | 0.344 | 0.177 | 0.256 | 0.223 |
| CPS67_4 | deep | deciduous | dystric Cambisol | 52 | 374 | 360 | 139 | 370 | 0.332 | 0.224 | 0.246 | 0.198 |
| EPC08_1 | surface | coniferous | entic Podzol | 23 | 270 | 260 | 193 | 351 | 0.348 | 0.253 | 0.228 | 0.170 |
| EPC34_1 | surface | coniferous | entic Podzol | 20 | 300 | 291 | 188 | 349 | 0.345 | 0.237 | 0.233 | 0.185 |
| EPC34_4 | deep | coniferous | entic Podzol | 38 | 150 | 143 | 181 | 362 | 0.336 | 0.300 | 0.177 | 0.186 |
| EPC39a_1 | surface | coniferous | eutric Cambisol | 30 | 237 | 228 | 209 | 346 | 0.367 | 0.270 | 0.189 | 0.174 |
| EPC71_1 | surface | coniferous | entic Podzol | 32 | 281 | 272 | 177 | 351 | 0.353 | 0.242 | 0.225 | 0.180 |

| | | | | | | | | | | | | |
|---|---|---|---|---|---|---|---|---|---|---|---|---|
| EPC73_1 | surface | coniferous | dystric Cambisol | 31 | 316 | 305 | 204 | 347 | 0.349 | 0.238 | 0.219 | 0.194 |
| EPC73_4 | deep | coniferous | dystric Cambisol | 53 | 170 | 164 | 165 | 363 | 0.343 | 0.288 | 0.197 | 0.171 |
| EPC81_1 | surface | coniferous | entic Podzol | 23 | 250 | 241 | 182 | 355 | 0.340 | 0.250 | 0.226 | 0.184 |
| EPC81_4 | deep | coniferous | entic Podzol | 46 | 138 | 132 | 203 | 364 | 0.338 | 0.279 | 0.207 | 0.176 |
| EPC87_1 | surface | coniferous | entic Podzol | 23 | 197 | 190 | 197 | 350 | 0.344 | 0.256 | 0.222 | 0.179 |
| EPC88_1 | surface | coniferous | dystric Cambisol | 22 | 326 | 315 | 185 | 347 | 0.373 | 0.225 | 0.224 | 0.179 |
| EPC88_4 | deep | coniferous | dystric Cambisol | 41 | 149 | 142 | 222 | 356 | 0.337 | 0.304 | 0.185 | 0.173 |
| HET03_1 | surface | deciduous | dystric Cambisol | 35 | 523 | 504 | 137 | 357 | 0.334 | 0.172 | 0.278 | 0.217 |
| HET03_4 | deep | deciduous | dystric Cambisol | 47 | 441 | 427 | 140 | 362 | 0.335 | 0.203 | 0.253 | 0.208 |
| HET04_1 | surface | deciduous | eutric Cambisol | 29 | 257 | 242 | 215 | 345 | 0.384 | 0.280 | 0.176 | 0.160 |
| HET04_4 | deep | deciduous | eutric Cambisol | 28 | 245 | 236 | 200 | 357 | 0.344 | 0.315 | 0.162 | 0.179 |
| HET09_4 | deep | deciduous | entic Podzol | 47 | 402 | 390 | 133 | 369 | 0.323 | 0.226 | 0.248 | 0.203 |
| HET14_1 | surface | deciduous | dystric Cambisol | 29 | 302 | 283 | 133 | 361 | 0.376 | 0.231 | 0.227 | 0.166 |
| HET14_4 | deep | deciduous | dystric Cambisol | 49 | 366 | 354 | 138 | 369 | 0.333 | 0.235 | 0.236 | 0.197 |
| HET21_1 | surface | deciduous | eutric Cambisol | 28 | 242 | 225 | 206 | 355 | 0.333 | 0.329 | 0.164 | 0.174 |
| HET21_4 | deep | deciduous | eutric Cambisol | 40 | 259 | 248 | 224 | 356 | 0.317 | 0.330 | 0.175 | 0.179 |
| HET25_1 | surface | deciduous | eutric Cambisol | 33 | 245 | 231 | 154 | 362 | 0.349 | 0.273 | 0.205 | 0.173 |
| HET25_4 | deep | deciduous | eutric Cambisol | 43 | 233 | 223 | 197 | 353 | 0.327 | 0.310 | 0.184 | 0.179 |
| HET26_1 | surface | deciduous | eutric Cambisol | 25 | 244 | 232 | 223 | 349 | 0.345 | 0.311 | 0.173 | 0.171 |
| HET26_4 | deep | deciduous | eutric Cambisol | 32 | 198 | 186 | 249 | 348 | 0.331 | 0.324 | 0.168 | 0.177 |
| HET30_1 | surface | deciduous | entic Podzol | 28 | 427 | 414 | 158 | 354 | 0.330 | 0.203 | 0.255 | 0.212 |
| HET30_4 | deep | deciduous | entic Podzol | 47 | 314 | 302 | 145 | 373 | 0.357 | 0.239 | 0.211 | 0.193 |
| HET52_1 | surface | deciduous | eutric Cambisol | 31 | 279 | 269 | 189 | 349 | 0.358 | 0.268 | 0.189 | 0.186 |
| HET52_4 | deep | deciduous | eutric Cambisol | 43 | 284 | 269 | 229 | 353 | 0.318 | 0.299 | 0.197 | 0.186 |
| HET54b_1 | surface | deciduous | eutric Cambisol | 30 | 277 | 267 | 192 | 351 | 0.340 | 0.276 | 0.198 | 0.186 |
| HET55_1 | surface | deciduous | entic Podzol | 38 | 441 | 430 | 125 | 363 | 0.378 | 0.191 | 0.242 | 0.188 |
| HET60_1 | surface | deciduous | eutric Cambisol | 22 | 300 | 288 | 212 | 346 | 0.338 | 0.296 | 0.186 | 0.180 |
| HET60_4 | deep | deciduous | eutric Cambisol | 39 | 295 | 277 | 202 | 355 | 0.351 | 0.293 | 0.189 | 0.166 |
| HET65_4 | deep | deciduous | dystric Cambisol | 60 | 277 | 261 | 132 | 383 | 0.314 | 0.249 | 0.242 | 0.194 |

| | | | | | | | | | | | | |
|---|---|---|---|---|---|---|---|---|---|---|---|---|
| HET81_1 | surface | deciduous | entic Podzol | 30 | 401 | 390 | 140 | 359 | 0.347 | 0.211 | 0.255 | 0.187 |
| HET81_4 | deep | deciduous | entic Podzol | 50 | 460 | 436 | 127 | 364 | 0.330 | 0.218 | 0.241 | 0.211 |
| HET88_1 | surface | deciduous | dystric Cambisol | 37 | 434 | 423 | 134 | 352 | 0.349 | 0.182 | 0.259 | 0.211 |
| HET88_4 | deep | deciduous | dystric Cambisol | 50 | 449 | 432 | 130 | 367 | 0.328 | 0.209 | 0.251 | 0.212 |
| MEL05_1 | surface | coniferous | eutric Cambisol | 29 | 204 | 196 | 247 | 341 | 0.366 | 0.253 | 0.203 | 0.178 |
| MEL05_4 | deep | coniferous | eutric Cambisol | 35 | 166 | 156 | 212 | 353 | 0.347 | 0.328 | 0.155 | 0.170 |
| PS04_4 | deep | coniferous | dystric Cambisol | 78 | 112 | 107 | 161 | 363 | 0.354 | 0.288 | 0.176 | 0.182 |
| PS15_1 | surface | coniferous | dystric Cambisol | 28 | 239 | 231 | 180 | 353 | 0.339 | 0.254 | 0.219 | 0.188 |
| PS41_1 | surface | coniferous | entic Podzol | 39 | 261 | 253 | 157 | 354 | 0.355 | 0.242 | 0.228 | 0.175 |
| PS41_4 | deep | coniferous | entic Podzol | 69 | 206 | 193 | 221 | 360 | 0.343 | 0.274 | 0.200 | 0.183 |
| PS63_1 | surface | coniferous | dystric Cambisol | 32 | 252 | 243 | 184 | 349 | 0.342 | 0.248 | 0.218 | 0.191 |
| PS63_4 | deep | coniferous | dystric Cambisol | 55 | 173 | 173 | 173 | 363 | 0.348 | 0.279 | 0.194 | 0.178 |
| PS67a_1 | surface | coniferous | entic Podzol | 26 | 292 | 283 | 177 | 348 | 0.360 | 0.230 | 0.234 | 0.176 |
| PS67a_4 | deep | coniferous | entic Podzol | 53 | 161 | 153 | 154 | 375 | 0.331 | 0.298 | 0.188 | 0.182 |
| PS67b_1 | surface | coniferous | entic Podzol | 71 | 284 | 276 | 162 | 348 | 0.360 | 0.231 | 0.227 | 0.182 |
| PS88_1 | surface | coniferous | entic Podzol | 37 | 285 | 276 | 182 | 348 | 0.354 | 0.236 | 0.224 | 0.186 |
| PS88_4 | deep | coniferous | entic Podzol | 67 | 223 | 214 | 134 | 374 | 0.323 | 0.264 | 0.210 | 0.203 |
| PS89_1 | surface | coniferous | entic Podzol | 37 | 283 | 274 | 192 | 348 | 0.355 | 0.210 | 0.250 | 0.185 |
| PS89_4 | deep | coniferous | entic Podzol | 66 | 188 | 178 | 212 | 362 | 0.370 | 0.257 | 0.194 | 0.179 |
| SP05_4 | deep | coniferous | eutric Cambisol | 50 | 111 | 106 | 231 | 355 | 0.323 | 0.340 | 0.179 | 0.158 |
| SP07_1 | surface | coniferous | entic Podzol | 26 | 343 | 332 | 201 | 345 | 0.338 | 0.225 | 0.240 | 0.197 |
| SP07_4 | deep | coniferous | entic Podzol | 48 | 241 | 230 | 175 | 373 | 0.309 | 0.286 | 0.206 | 0.200 |
| SP09_4 | deep | coniferous | entic Podzol | 47 | 285 | 261 | 196 | 358 | 0.316 | 0.271 | 0.231 | 0.181 |
| SP11_1 | surface | coniferous | eutric Cambisol | 38 | 223 | 215 | 216 | 344 | 0.370 | 0.264 | 0.193 | 0.172 |
| SP11_4 | deep | coniferous | eutric Cambisol | 42 | 166 | 157 | 259 | 351 | 0.327 | 0.325 | 0.176 | 0.172 |
| SP25_1 | surface | coniferous | eutric Cambisol | 33 | 207 | 200 | 193 | 347 | 0.362 | 0.260 | 0.194 | 0.184 |
| SP25_4 | deep | coniferous | eutric Cambisol | 43 | 170 | 160 | 251 | 354 | 0.324 | 0.306 | 0.196 | 0.174 |
| SP26_1 | surface | coniferous | eutric Cambisol | 29 | 209 | 202 | 199 | 349 | 0.343 | 0.286 | 0.186 | 0.185 |
| SP26_4 | deep | coniferous | eutric Cambisol | 42 | 197 | 183 | 233 | 352 | 0.356 | 0.291 | 0.180 | 0.174 |

| | | | | | | | | | | | | |
|---|---|---|---|---|---|---|---|---|---|---|---|---|
| SP38_1 | surface | coniferous | dystric Cambisol | 27 | 234 | 226 | 171 | 353 | 0.346 | 0.247 | 0.217 | 0.191 |
| SP38_4 | deep | coniferous | dystric Cambisol | 57 | 166 | 151 | 177 | 366 | 0.323 | 0.291 | 0.201 | 0.184 |
| SP39_1 | surface | coniferous | eutric Cambisol | 28 | 194 | 187 | 206 | 351 | 0.346 | 0.290 | 0.186 | 0.177 |
| SP39_4 | deep | coniferous | eutric Cambisol | 36 | 181 | 163 | 233 | 352 | 0.332 | 0.296 | 0.191 | 0.181 |
| SP57_4 | deep | coniferous | dystric Cambisol | 47 | 233 | 221 | 190 | 364 | 0.324 | 0.272 | 0.214 | 0.190 |
| SP63_1 | surface | coniferous | dystric Cambisol | 24 | 334 | 324 | 182 | 346 | 0.341 | 0.224 | 0.235 | 0.199 |
| SP68_1 | surface | coniferous | dystric Cambisol | 30 | 258 | 251 | 187 | 347 | 0.356 | 0.245 | 0.214 | 0.186 |
| SP68_4 | deep | coniferous | dystric Cambisol | 57 | 139 | 133 | 188 | 367 | 0.338 | 0.291 | 0.205 | 0.166 |

**Table C.1**. Distribution of the 86 POM samples considered in this study among the various classes of depth (surface and deep layers; 0–10 cm and 40–80 cm), soil (dystric Cambisol, eutric Cambisol, entic Podzol) and vegetation (coniferous and deciduous).

| | 0–10 cm | 40–80 cm | coniferous | deciduous |
|---|---|---|---|---|
| dystric Cambisol | 15 | 15 | 14 | 16 |
| eutric Cambisol | 15 | 14 | 12 | 17 |
| entic Podzol | 16 | 11 | 19 | 8 |
| *total* | | | *45* | *41* |
| coniferous | 24 | 21 | | |
| deciduous | 22 | 19 | | |
| *total* | *46* | *40* | | |

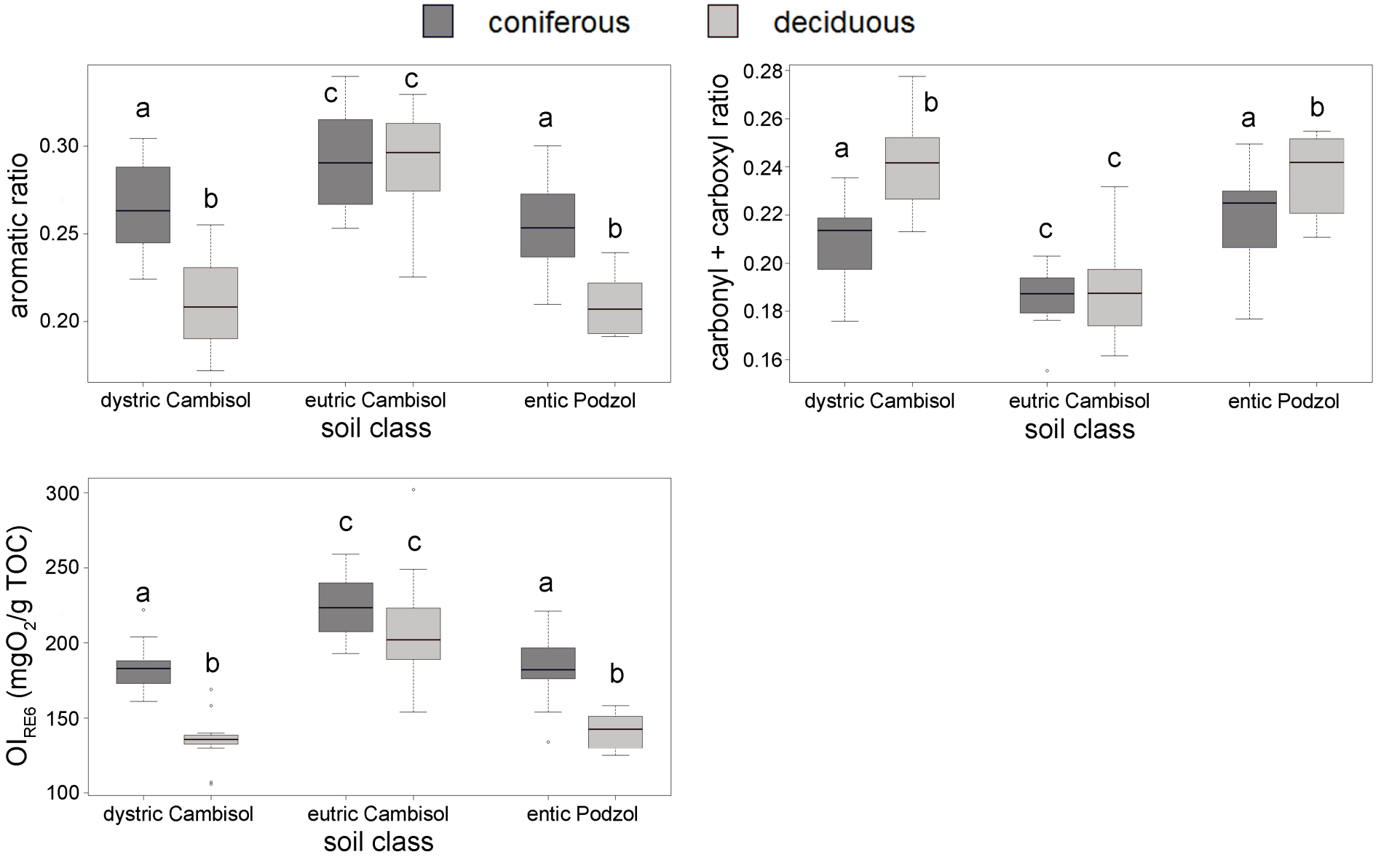
coniferous
deciduous
aromatic ratio
0.30
0.25
0.20
a
b
c
c
a
b
dystric Cambisol
eutric Cambisol
entic Podzol
soil class
carbonyl + carboxyl ratio
0.28
0.26
0.24
0.22
0.20
0.18
0.16
a
b
c
c
a
b
dystric Cambisol
eutric Cambisol
entic Podzol
soil class
$OI_{RE6}$ ($mgO_2/g$ TOC)
300
250
200
150
100
a
b
c
c
a
b
dystric Cambisol
eutric Cambisol
entic Podzol
soil class

**Table E.1.** Table of correlations for all samples and for each layer individually between the POM chemical properties (C/N ratio, ether + alcohol ratio, aromatic ratio, carbonyl + carboxyl ratio, aliphatic ratio) and POM thermal stability (HI corrected, $OI_{RE6}$, $T_{50\_CO2\_PYR}$). Significance is indicated as follows: ***: $p < 0.001$; **: $p < 0.01$; *: $p < 0.05$. The high (> 0.6) correlations between parameters derived from different methods are marked in bold. n = 86 for all layers; n = 46 for surface layer and n = 40 for deep layer, respectively.

**ALL LAYERS**

| | C/N ratio | ether + alcohol ratio | aromatic ratio | carbonyl + carboxyl ratio | aliphatic ratio | HI corrected | $OI_{RE6}$ |
|---|---|---|---|---|---|---|---|
| ether + alcohol ratio | −0.35*** | | | | | | |
| aromatic ratio | 0.19 | −0.44*** | | | | | |
| carbonyl + carboxyl ratio | −0.07 | 0.08 | **−0.88*** ** | | | | |
| aliphatic ratio | 0.08 | −0.21 | **−0.63*** ** | **0.64*** ** | | | |
| HI corrected | −0.25* | 0.25* | **−0.83*** ** | **0.75*** ** | **0.65*** ** | | |
| $OI_{RE6}$ | −0.21 | −0.07 | **0.67*** ** | **−0.70*** ** | −0.59*** | −0.56*** | |
| $T_{50\_CO2\_PYR}$ | **0.68*** ** | −0.45*** | 0.07 | 0.09 | 0.20 | −0.05 | −0.46*** |

**SURFACE LAYER**

| | C/N ratio | ether + alcohol ratio | aromatic ratio | carbonyl + carboxyl ratio | aliphatic ratio | HI corrected | $OI_{RE6}$ |
|---|---|---|---|---|---|---|---|
| ether + alcohol ratio | 0.19 | | | | | | |
| aromatic ratio | −0.15 | −0.29 | | | | | |
| carbonyl + carboxyl ratio | 0.13 | −0.03 | **−0.87*** ** | | | | |
| aliphatic ratio | 0.12 | −0.31* | **−0.62*** ** | **0.60*** ** | | | |
| HI corrected | 0.03 | 0.15 | **−0.87*** ** | **0.78*** ** | **0.62*** ** | | |
| $OI_{RE6}$ | −0.28 | −0.20 | **0.75*** ** | **−0.69*** ** | −0.42** | **−0.65*** ** | |
| $T_{50\_CO2\_PYR}$ | 0.17 | −0.25 | −0.16 | 0.31* | 0.10 | 0.14 | **−0.65*** ** |

**DEEP LAYER**

| | C/N ratio | ether + alcohol ratio | aromatic ratio | carbonyl + carboxyl ratio | aliphatic ratio | HI corrected | $OI_{RE6}$ |
|---|---|---|---|---|---|---|---|
| ether + alcohol ratio | 0.07 | | | | | | |
| aromatic ratio | −0.43** | −0.17 | | | | | |
| carbonyl + carboxyl ratio | 0.41** | −0.22 | **−0.87*** ** | | | | |
| aliphatic ratio | 0.25 | −0.24 | **−0.77*** ** | **0.74*** ** | | | |
| HI corrected | −0.07 | −0.05 | **−0.71*** ** | **0.65*** ** | **0.71*** ** | | |
| $OI_{RE6}$ | −0.59*** | 0.06 | **0.70*** ** | **−0.70*** ** | **−0.71*** ** | −0.46** | |
| $T_{50\_CO2\_PYR}$ | **0.65*** ** | −0.02 | **−0.62*** ** | **0.63*** ** | 0.55*** | 0.24 | **−0.79*** ** |